

Operation Control and Analysis of Hybrid Multiterminal HVDC System Using Different Control Strategies under Abnormal Conditions



By

Syed Tahir Shah

Reg # 00000206189

Session 2017-19

Supervised by

Asst. Prof. Dr. Abraiz Khattak

**A Thesis Submitted to the US-Pakistan Center for Advanced
Studies in Energy in partial fulfilment of the requirements for the
degree of**

**MASTERS of SCIENCE in
ELECTRICAL ENGINEERING (POWER)**

US-Pakistan Center for Advanced Studies in Energy (USPCAS-E)

National University of Sciences and Technology (NUST)

H-12, Islamabad 44000, Pakistan

January 2021

Operation Control and Analysis of Hybrid Multiterminal HVDC System Using Different Control Strategies under Abnormal Conditions



By

Syed Tahir Shah

Reg # 00000206189

Session 2017-19

Supervised by

Asst. Prof. Dr. Abraiz Khattak

**A Thesis Submitted to the US-Pakistan Center for Advanced
Studies in Energy in partial fulfilment of the requirements for the
degree of**

**MASTERS of SCIENCE in
ELECTRICAL ENGINEERING (POWER)**

US-Pakistan Center for Advanced Studies in Energy (USPCAS-E)

National University of Sciences and Technology (NUST)

H-12, Islamabad 44000, Pakistan

January 2021

THESIS ACCEPTANCE CERTIFICATE

It is certified that final copy of MS/MPhil thesis written by **Mr. Syed Tahir Shah** (Registration No. **00000206189**) of US-Pakistan Center for Advanced Studies in Energy (USPCAS-E) has been vetted by undersigned, found complete in all respects as per NUST Statues/Regulations, is within similarity indices limit, errors and mistakes, and is accepted as partial fulfilment for award of MS/MPhil degree. It is further certified that necessary amendments as pointed out by GEC members of the scholar have also been incorporated in the said thesis.

Signature: _____

Name of Supervisor Dr. Abraiz Khattak

Date: _____

Signature (HoD): _____

Date: _____

Signature (Dean/Principal): _____

Date: _____

Certificate

This is to certify that work in this thesis has been carried out by **Mr. Syed Tahir Shah** and completed under my supervision in US-Pakistan Center for Advanced Studies in Energy (USPCAS-E), National University of Sciences and Technology, H-12, Islamabad, Pakistan.

Supervisor:

Dr. Abraiz Khattak
USPCAS-E
NUST, Islamabad

GEC member # 1:

Dr. Kashif Imran
USPCAS-E
NUST, Islamabad

GEC member # 2:

Dr. Abasin Ulasyar
USPCAS-E
NUST, Islamabad

GEC member # 3:

Dr. Hassan Abdullah
USPCAS-E
NUST, Islamabad

HoD

Dr. Kashif Imran
USPCAS-E
NUST, Islamabad

Principal/ Dean

Dr. Adeel Waqas
USPCAS-E
NUST, Islamabad

Acknowledgment

I would like to thank and acknowledge all those who helped me with the completion of this thesis.

Foremost, I would like to acknowledge my Supervisor **Dr. Abraiz Khattak** for his keen support, Insight to core knowledge and advices.

Besides my Supervisor, I would also like to appreciate the Guidance and Examination Committee Members **Dr. Kashif Imran, Dr. Abasin Ulasyar and Dr. Hassan Abdullah** for their valuable comments and active participation.

My sincere thanks to **Engr. Mr. Saeed and Mr. Kashif Janjua** for their valuable time and arrangement of Software.

At last, I would like to thank my family and friends too for their moral support during my research work.

ABSTRACT

HVDC transmission system technologies are becoming more suitable for integration of clean energy sources with improved reliability, security, efficient controllability and desirable stability. It has also been made cost effective for several applications of power transfer usually beyond a certain distance and higher power ratings. Most of the HVDC links being deployed these days are LCCs and VSCs with two level and multi-modular level conversion technologies. The advancements in the interoperability of these technologies with both AC and DC systems has given rise to the application of MTDC systems. Moreover, the pressures from the international communities to decrease greenhouse gases, has forced scientific community all over the globe to bring effective technologies in the market, to replace over the counter carbon di oxide emitting technologies. For the above reasons the focus has also shifted towards using MTDC systems. However this technology is not yet fully matured yet, and requires state of the art research and analysis. Recent research studies have stressed over, developing non Hybrid HVDC grids based on only single type of converter technologies. However, this research work explores the performance of a proposed scenario for integrating different systems using a Hybrid LCC-MMC type MTDC scheme with the use of DC-DC converter. Furthermore, the topological analysis of the scheme, also requires scrutiny during different abnormal conditions to improve the reliability of the grids. The systems startup schemes and performance under specific faulty conditions are also compared using the integration of virtual energy sources and incorporating different HVDC networks with DC-DC converters. The multiple advantages from the in-depth analysis have been highlighted in detail in the thesis ahead.

Keywords: High Voltage Direct Current (HVDC), Line Commutated Converters (LCC), Voltage Source Converter (VSC), Multi-Terminal Direct Current.

Table of Contents

1	Chapter 1: Introduction	1
1.1	<i>Background: -.....</i>	<i>1</i>
1.2	<i>State of the art Hybrid Multi-terminal HVDC systems: -</i>	<i>2</i>
1.3	<i>Motivation and contributions: -</i>	<i>3</i>
1.4	<i>Thesis Layout: -.....</i>	<i>4</i>
	<i>References</i>	<i>5</i>
2	Chapter 2: Literature Review	7
2.1	<i>HVDC System Configurations.....</i>	<i>7</i>
2.1.1	Monopole Link.....	7
2.1.2	Bipolar Link	7
2.1.3	Homopolar Link	8
2.1.4	Point to Point Links.....	8
2.1.5	Back to Back Links	9
2.1.6	Multiterminal Link.....	9
2.2	<i>MTDC grid.....</i>	<i>10</i>
2.3	<i>MTDC grid Topologies</i>	<i>10</i>
2.3.1	Radial Network	12
2.3.2	Ring Network	12
2.3.3	Meshed Network	13

2.4	<i>Line Commutated Converters</i>	13
2.4.1	Introduction	13
2.4.2	Thyristors (Operation not included?)	13
2.4.3	Converter Configuration	14
2.4.4	Advantages and Applications.....	16
2.5	<i>Voltage Source Converters:</i>	17
2.5.1	Introduction:	17
2.5.2	IGBT (Operation Included or not):	18
2.5.3	Two-level converter:	18
2.5.4	Three Level Converter:	19
2.6	<i>Modular Multilevel Converters:</i>	21
2.6.1	Module Topologies:	22
2.7	<i>Hybrid Converters:</i>	22
2.8	<i>DC to DC Converters in HVDC</i>	24
2.9	<i>Abnormal Conditions</i>	25
	<i>References</i>	26
3	Chapter 3: Modeling Control and Operation of HVDC Converters	27
3.1	<i>Modeling Control and Operation of LCC HVDC grids</i>	27
3.1.1	Operational Characteristics of LCC HVDC.....	27
3.1.2	Ideal Steady State Characteristics:	28

3.1.3	Actual Steady state Characteristics and Basic Control Strategies of LCC.....	29
3.2	<i>Modeling Control and Operation of VSC HVDC grids</i>	31
3.2.1	Modeling of VSC Station.....	31
3.2.2	Control of VSC station:.....	32
3.2.3	Inner Vector Current control Loop:	33
3.2.4	Outer Control Loop:.....	34
3.3	<i>Modeling Control and Operation of MMC HVDC grids</i>	36
3.3.1	Modeling of MMC station	36
3.3.2	Control Structure of MMC station	38
4	Chapter 4: Proposed Case study for Hybrid MTDC Grid	40
	<i>References</i>	43
5	Chapter 5: Results and Analysis	44
5.1	<i>Grid Start-Up Schemes</i>	44
5.2	<i>AC voltage Sags</i>	46
5.3	<i>DC voltage Sags</i>	50
	Chapter 6: Conclusion	53

List of Figures

Figure 1.1: World energy sources usage over the course of 200 years.....	1
Figure 1.2: HVDC VS HVAC Cost Benefit Analysis Graph	2
Figure 1.3: Available power resources and projected North Sea interconnection with Euro-African super grid	3
Figure 2.2: Bipole HVDC link.....	7
Figure 2.3: Homopole HVDC link.....	8
Figure 2.4: Point-Point HVDC link.	8
Figure 2.5: Back-Back HVDC link.....	9
Figure 2.6: Series-Parallel, Multi-terminal HVDC link.....	9
Figure 2.7: North-Sea Multi-terminal HVDC Example.....	10
Figure 2.8: 4-terminal Series-Parallel LCC type HVDC Connection.....	11
Figure 2.9: Radial MTDC network topology.....	12
Figure 2.10: Circular MTDC network topology.	12
Figure 2.11: Meshed MTDC network topology.....	13
Figure 2.12: Structure and Symbol for (a) diode and (b) thyristor.	14
Figure 2.13: Six pulse converter configuration for LCC HVDC.....	14
Figure 2.14: Working Principle of Six pulse converter for LCC HVDC.....	15
Figure 2.15 Valve waveforms of DC voltages.....	15
Figure 2.16: Twelve Pulse converter configuration for LCC HVDC.....	16

Figure 2.17: Symbol of IGBT circuit.....	18
Figure 2.18: Two level Six pulse VSC HvdC converter configuration.	18
Figure 2.19: Internal valve circuitry (Too and fro switch).....	19
Figure 2.20: Three Level VSC HVDC converter configuration with antiparallel diodes.	20
Figure 2.22: One Phase leg of VSC HVDC converter with (a) two levels, (b) three levels, (c) five levels.	21
Figure 2.24: Switching module (SM) topologies: (a) half bridge; (b) full bridge.	22
Figure 2.25: Three terminal Hybrid HVDC transmission system.....	23
Figure 2.26: Four-terminal Bipolar Hybrid HVDC transmission system.....	23
Figure 2.27: Dual-infeed Hybrid dual-infeed HVDC transmission system.....	24
Figure 2.28: DC-DC Proposed classification for HVDC converters application flow chart.....	24
Figure 3.1: HVDC Transmission link (a) schematic diagram, (b) equivalent circuit, (c) voltage profile.....	27
Figure 3.2: Ideal steady state characteristics.....	28
Figure 3.3: Alpha and gamma characteristics based rectifier and inverter modes.....	29
Figure 3.4: Actual steady state characteristics of voltage and current for a two terminal LCC HVDC system.	29
Figure 3.5: Rectifier and Inverter Controller schematics.....	30
Figure 3.6: One phase schematic diagram of VSC two terminal HVDC link	31
Figure 3.7: AC and DC side Modelling of VSC system.....	32

Figure 3.8: Complete control strategy for VSC HVDC system.....	33
Figure 3.9: Inner control loop modeling of VSC converter.....	34
Figure 3.10: Open loop control of (a) active and (b) reactive power controllers.....	35
Figure 3.11: Modeling of complete control system of inner and outer controls.....	35
Figure 3.12: Representation of detailed Arm Average Model of a MMC converter.	36
Figure 3.13: Equivalent circuit of each AAM phase.....	37
Figure 3.14: Simplified MMC model circuit in dq0 reference frame.....	37
Figure 3.15: Block diagram modeling of complete MMC physical system.	38
Figure 3.16: DC current loop modelling of MMC converter.....	38
Figure 3.17: Total energy control modelling of MMC converter.	39
Figure 3.18: Complete physical model of outer and inner control of MMC converter.	39
Figure 4.1: Proposed seven terminal MTDC Hybrid LCC-MMC HVDC Circuit Model.	41
Figure 4.2: HVDC networks divided into network zones on the basis of HVDC grid types.	42
Figure 5.1: System response during start-up under normal conditions: (a) DC voltages (b) AC voltages (c) DC currents (d) reactive powers	45
Figure 5.2: System response during start-up with DC source integration (a) DC voltages (b) AC voltages (c) DC currents	45
Figure 5.3: System response during unbalanced AC voltage Sags without DC source Integration: (a) DC voltages (b) AC voltages (c) DC currents (d) reactive powers.	47

Figure 5.4: System response during balanced AC voltage Sags without DC source Integration: (a) DC voltages (b) AC voltages (c) DC currents (d) reactive powers.	49
Figure 5.5: System response during start-up unbalanced AC voltage Sags with DC source Integration: (a) DC voltages (b) AC voltages (c) DC currents (d) reactive powers.	50
Figure 5.6: System response during DC voltage Sags at B3 (a) DC voltages (b) AC voltages (c) DC currents (d) reactive powers.....	51
Figure 5.7: System response during DC voltage Sags at F1: (a) DC voltages (b) AC voltages	52
Figure 5.8: System response during DC voltage Sags at F1 (Connection Topology) (a) DC voltages (b) AC voltages.....	52

List of Tables

Table. 1: Characteristics of series and parallel LCC HVDC connection	11
Table. 2: Advantages and applications of LCC HVDC system.....	17
Table. 3: System Data for AC and DC grids and Converters.	411
Table. 4: Max change in DC voltage and Peak increase in AC current at 4 converters.	488

List of Abbreviations

CO ₂	Carbon Die Oxide
LCC	Line Commutated Converters
VSC	Voltage Source Converters
MMC	Multilevel Modular Converters
HVDC	High Voltage Direct Current
HVAC	High Voltage Alternating
MTDC	Multiterminal Direct Current
HMTDC	Hybrid Multiterminal
PTP	Point to Point

B2B	Back to Back
IGBT	Insulated Gate Bipolar Transistor
MOSFET	Metal Oxide Field Effect Transistors
BJT	Bipolar Junction Transistor
PWM	Pulse Width Modulation
THD	Total Harmonic Distortion
PLL	Phase Locked Loop
PCC	Point of Common Coupling

Chapter 1: Introduction

1.1 Background: -

The consumption of electricity on day to day basis is ever-growing. Today, more than 85% of the people in the world have access to electricity. However, this electricity comes from both renewable and non-renewable energy sources, mostly from non-renewables as shown in the Fig.1 [1]. The dependency on these CO2 emitting sources, is facing reluctance from societies mainly due to the distress over environmental hazards. The current transmission system is constantly being reshaped to overcome multiple challenges related to integration of different systems. These include interconnecting, large offshore renewable energy sources, bulk power resources from thousands of Kilometers to the mainland, while other challenges include integration of Passive resources and adaptive power flow controls for DC grids. Due to the advancements in the development of HVDC converters and the vast variety of advantages provided by the HVDC systems, in the recent years HVDC technology is used as an alternative for HVAC technology to prevail over these challenges. The conventional HVAC transmission system is limited to transmitting power over several kilometers and hence requires more reactive power compensation devices which increases costs and losses in the system [2]. On the other hand HVDC based transmission systems are based on five main objectives.

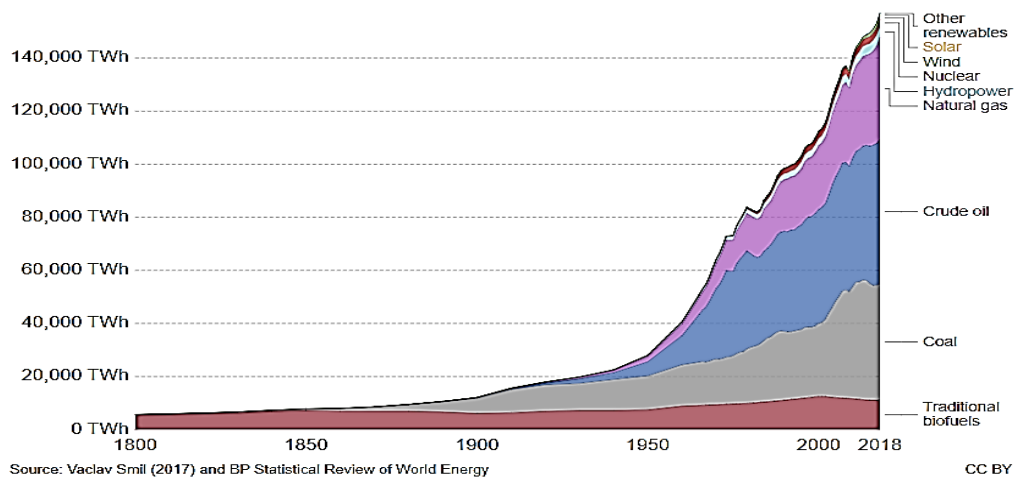


Figure 1.1: World energy sources usage over the course of 200 years.

- I. Interconnecting Offshore Energy Farms through subsea cables (Wind Farms, Solar Farms and Oil Fields)
- II. Transferring bulk power from onshore sites (Wind/ Solar/ Coal and Hydel)
- III. Interconnecting Asynchronous or Passive systems
- IV. Cost Benefits (After break even distance as shown in Fig. 1.2 [3])
- V. Inter-countries Energy Markets or supergrids (European Grid, Euro-African Grid, Asian Grid as shown in Fig. 1.3)

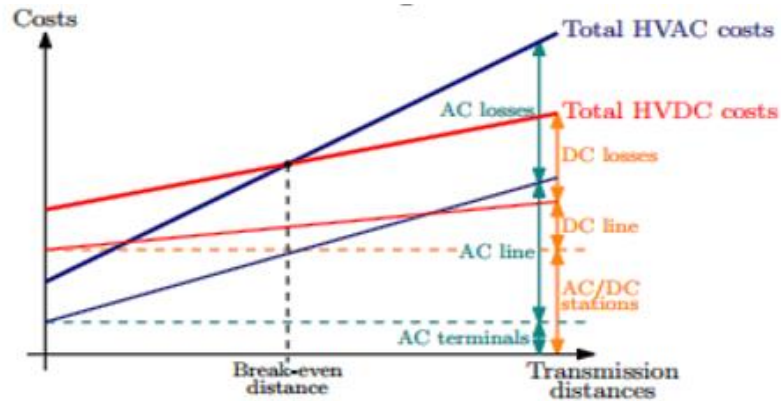


Figure 1.2: HVDC VS HVAC Cost Benefit Analysis Graph

1.2 State of the art Hybrid Multi-terminal HVDC systems: -

More and more point to point HVDC links have been deployed in China, Europe and India. Earlier the HVDC systems were limited to mostly two terminal links using Line Commutated Converter LCC-HVDC systems, but with the advancements in Power Electronic converters like Voltage Source Converter VSC-HVDC and Multilevel Modular Converter MMC based HVDC systems, the case of interconnecting more offshore renewable sources with improved interconnecting capabilities, has been made possible [4]. This opened the gateway for HVDC grids composing of more than two terminal HVDC stations known as Multiterminal High Voltage DC systems (MTDC), [5]. As the HVDC grids are either made up of LCC or VSC type converter technology, a Hybrid (LCC-VSC) type system [6] holds much greater challenges and growth from the application point of view. LCC MTDC grids have been operational since 1992 when Quebec-New England HVDC Transmission [7] was extended to three terminal system from a two terminal system. VSC MTDC grids have been around since 1999 in Shin-Shinano HVDC in Japan [8] which was made up of a back to back three terminal system, however the application of this system is fairly different that is interconnecting systems with different frequencies. In

recent days, more MTDC network possibilities have been recognize. The development of MMC converters has let the operational capabilities of MTDC networks more convenient [9]. More MTDC networks using MMC HVDC systems are planned for tapping into the transfer of offshore renewable energy to the mainland. Using the notion that, many LCC-HVDC links are already operational and more VSC (MMC)-HVDC links will be installed for different applications and scenarios, such as Interconnecting the North Sea [10], euroafrican grid [11], a Hybrid MTDC system has yet to be matured and requires a lot of research. There are multiple aspects related to the interconnection challenges and operational issues that needs to be addressed.

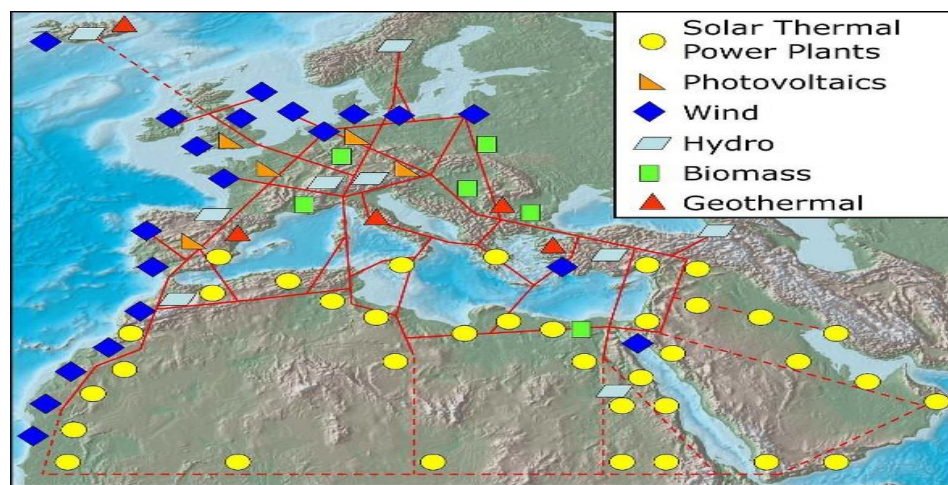


Figure 1.3: Available power resources and projected North Sea interconnection with Euro-African super grid

1.3 Motivation and contributions: -

Despite the attention given to the advantages of VSC MTDC and LCC MTDC grids, rare research has been conducted to investigate the prospects of Hybrid MTDC grids and their applications. In previous research studies, the use of DC-DC converter to connect DC sources, hybrid system and its impacts on overall DC grid's system performance is barely scrutinized. Moreover, the effects of interconnecting islanded load networks to the DC grid using MMC converters are also considered in this study. Furthermore, this thesis contributes to analyze the impacts of AC and DC faults on the DC grid's performance, also provides a new topological approach to interconnect remote area loads with the DC grid.

1.4 Thesis Layout: -

Chapter 1

This chapter includes the Introduction to the topic and defines the motive and objective behind the Thesis theme selection.

Chapter 2

Literature Review is presented here. The basic concepts of HVDC technologies have been discussed, which includes the Converter types, converter topologies, and faults in MTDC systems, and HVDC system configurations. A brief description about the working principles of Line Commutated (LCC), Voltage Source (VSC) and Multilevel Modular converters (MMC) is written. Furthermore the applications and concepts of DC-DC converters for MTDC systems is also explored.

Chapter 3

This chapter focuses on the modeling, operation and control of all three types of basic HVDC converters. First the modeling and operational characters of LCC-HVDC system is discussed followed by the control design of rectifier and inverter of LCC converter. Later the latest model and control designs for a two level VSC and a three level MMC is acquired.

Chapter 4

Proposed model for case study and its system description is provided in this chapter.

Chapter 5

In this chapter Results and Analysis for the system behavior during multiple conditions are presented with PSCAD based simulations.

Chapter 6

This chapter concludes the thesis work.

References

- [1] <https://socialistincanada.ca/ecology-newsroll/global-primary-energy-consumption-1850-to-2017/>
- [2] O. E. ONI, I. E. DAVIDSON, AND K. N. MBANGULA, "A REVIEW OF LCCHVDC AND VSC-HVDC TECHNOLOGIES AND APPLICATIONS," IN 2016 IEEE 16TH INTERNATIONAL CONFERENCE ON ENVIRONMENT AND ELECTRICAL ENGINEERING (EEEIC), 2016, PP. 1–7.
- [3] <https://electrical-engineering-portal.com/analysing-the-costs-of-high-voltage-direct-current-hvdc-transmission>
- [4] N. FLOURENTZOU, V. G. AGELIDIS, AND G. D. DEMETRIADES, "VSC-BASED HVDC POWER TRANSMISSION SYSTEMS: AN OVERVIEW," IEEE TRANS. IND. APPL., VOL. 24, PP. 592-602, 2009.
- [5] NAUSHATH MH, RAJAPAKSE AD, GOLE AM ET AL (2017) ENERGIZATION AND REGULATION OF A HYBRID HVDC GRID WITH LCC AND VSC. IEEE ELECTRICAL POWER AND ENERGY CONFERENCE (EPEC), SASKATOON, SK, CANADA, 22-25 OCT. 2017,6P.
- [6] BAKAS P, HARNEFORS L, NORRGA S ET AL (2016) A REVIEW OF HYBRID TOPOLOGIES COMBINING LINE-COMMUTATED AND CASCADED FULL-BRIDGE CONVERTERS. IEEE TRANSACTIONS ON POWER ELECTRONICS, 2016, 32(10):7435-7448.
- [7] The HVDC Transmission Québec - New England. <http://www.abb.com/industries/ap/db0003db004333/87f88a41a0be97afc125774b003e6109.aspx>, May 2012.
- [8] T. Nakajima, S. Irokawa. A Control System for HVDC Transmission by Voltage Sourced Converters. In Proceedings of 1999 IEEE PES Summer Meeting, volume 2, pages 1113–1119, 18-22 July 1999

- [9] RAULT, P. (2014). DYNAMIC MODELING AND CONTROL OF MULTI-TERMINAL HVDC GRIDS. PHD THESIS, LABORATORY L2EP, UNIVERSITY LILLE NORD-DE-FRANCE.
- [10] European Commission, “ENERGY Projects of common interest - Interactive map.” PLATTS for the underlying grids for electricity, gas and oil, 2018; European Union, 2018 [Online]. Available: http://ec.europa.eu/energy/infrastructure/transparency_platform/mapviewer/main.html#&ui-state=dialog. [Accessed: Feb. 25, 2019]
- [11] European Commission, “ENERGY Projects of common interest - Interactive map.” PLATTS for the underlying grids for electricity, gas and oil, 2018; European Union, 2018 [Online]. Available: http://ec.europa.eu/energy/infrastructure/transparency_platform/mapviewer/main.html#&ui-state=dialog. [Accessed: Feb. 25, 2019]

Chapter 2: Literature Review

2.1 HVDC System Configurations

2.1.1 Monopole Link

A Monopole connection is made up of either one or two six pulse converters with two terminals one is connected to a transmission line and the other with ground to provide return path for current. A metallic wire may also be used where earth resistivity is very high. In Subsea system the water is used as a return path. The cost of this configuration is low which attracts the use of such configurations also this system can be extended to bipolar connections easily.

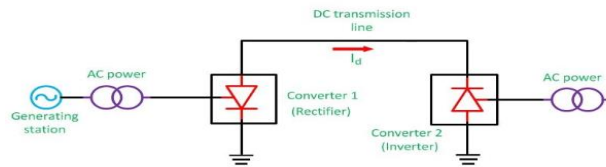


Figure 2.1: Monopole HVDC link.

2.1.2 Bipolar Link

A Bipolar configuration is made up of two transmission lines with either one or two twelve pulse converters. One transmission line connects the positive polarity of rectifier and inverter and the other transmission line connects with the negative polarity. This configuration is not cost effective as compared to monopolar links but proves to be more reliable under faulty conditions. The midpoints of both rectifier and inverter is connected via an electrode which provides an advantage of a monopole operation by using ground as a return path and the faulty converters.

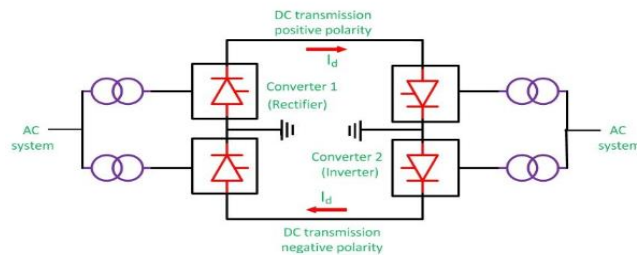


Figure 2.1: Bipole HVDC link.

2.1.3 Homopolar Link

A Homopolar configuration is made similar to bipolar having two conductors and a metallic return but the system only operates in negative polarity. This is done to reduce the effects of corona. The converters are arranged in parallel to attain the benefits of low insulation costs. Such links are not presently used due to complex nature of the configuration of converters.

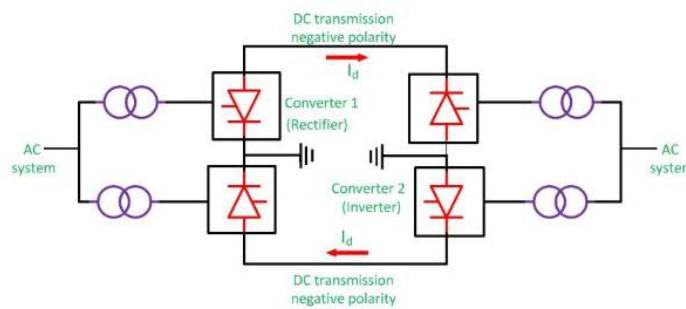


Figure 2.2: Homopole HVDC link.

2.1.4 Point to Point Links

This Configuration is made for mainly the purpose of connecting two or more asynchronous systems located at different areas. This only allows unidirectional power flow as shown in the Fig. 2.4.

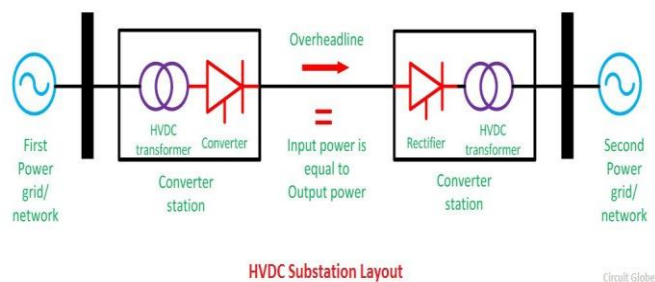


Figure 2.3: Point-Point HVDC link.

2.1.5 Back to Back Links

This configuration can be made from a Monopolar or bipolar link connected together using a single ground path. A back to back link is used for conversions between two asynchronous systems hence provides the advantage of coupling two or more electrical grids with different frequencies. This type of configuration is beneficial for inter-country or inter-continental HVDC transmission links. Its converters are located at the same location thus no transmission line is required.

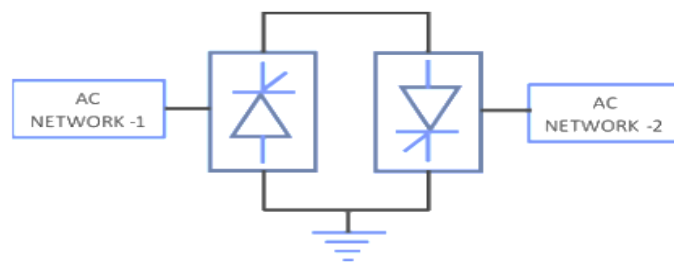


Figure 2.4: Back-Back HVDC link.

2.1.6 Multiterminal Link

A Complex network of three or more than three converters connected together combining the benefits of series and parallel network connections is known as a multiterminal link. Such a system is difficult to understand due to the applicability of different types of converter systems is discrete. Recently only two multiterminal systems are operational. The reversal of power can be easily achieved thus providing vast applications for the future HVDC technologies.

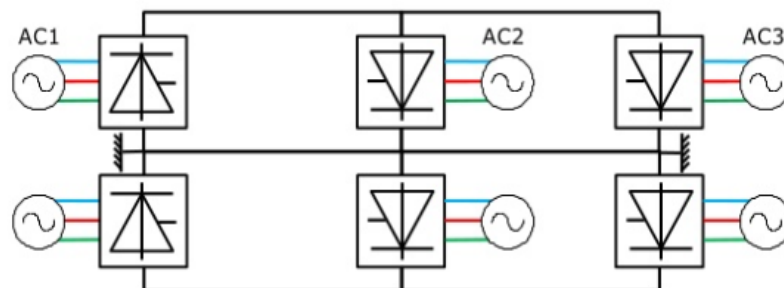


Figure 2.5: Series-Parallel, Multi-terminal HVDC link.

2.2 MTDC grid

Currently most of the HVDC connections are two terminal point to point transmission systems. A Multiterminal HvdC (MTDC) grid can be constructed from interconnecting more than two HVDC links as shown in Fig. 2.7. An MTDC is an alternative for the AC grid to transmit energy from remote area wind and solar farms or traditional power plants to the AC networks. The advantages provided by VSC HVDC systems has enabled the use of MTDCs on account for the improvements in scalability, flexibility, reliability and stability of the power system. However, with the increasing number of nodes and terminals the control strategies are becoming complex. An MTDC can also be formed by connecting different type of HVDC converter technologies such as a combination of LCC, VSC and MMCs which combines the advantages of all these converters technologies. The control strategies vastly depends upon the connection topologies.



Figure 2.6: North-Sea Multi-terminal HVDC Example.

2.3 MTDC grid Topologies

There are mainly two types of MTDC grid topologies, a series or a parallel connection of more than two links as shown in Fig. 2.8. Both have their limitations and advantages. A series connection can be further expanded into a radial and ring network or a hybrid connection. Similarly a parallel connection can be expanded into a radial and a meshed or respectively hybrid connection of both. All types of topologies are dependent on the requirements and applications. Future MTDCs are supposed to be made up of different grid topologies with different converter topologies

according to the grid requirements, which poses a great need for the research and development of different control strategies and control designing for such topologies. Some of the basic properties of series and parallel MTDC connections are discussed below.

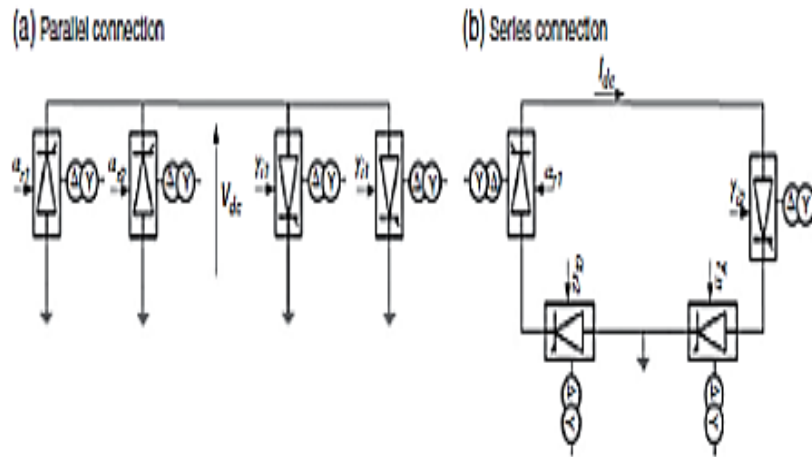


Figure 2.7: 4-terminal Series-Parallel LCC type HVDC Connection.

Table. 1: Characteristics of series and parallel LCC HVDC connection

S.NO	Parallel Connection	Series Connection
1	DC voltage at all Converters is same.	DC current at all converters is same.
2	One Big terminal controls DC voltage while other small terminals controls local DC currents.	Vice Versa.
3	Fast power reversal is not possible at any terminal.	Power reversal can be achieved.
4	A DC voltage fault will affect all converters.	A dc side fault will only interrupt a small amount of power.
5	Attractive for Multiterminal HVDC.	Attractive for small taps connections.

2.3.1 Radial Network

The advantage of this topology is the simplicity of control strategy. In this type of topology the voltage stability depends on the central station making it easy to control the rest of the system. The limitations exist when the central station fails and the power transfer is stopped to the rest of the system as there is no other path for power to flow.

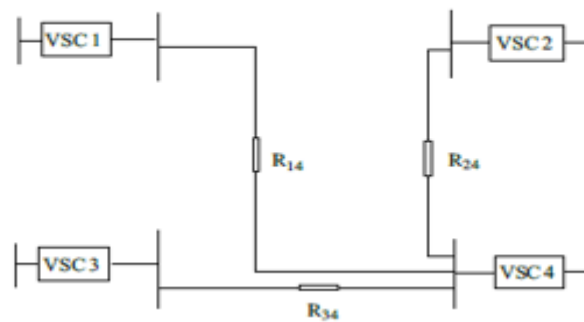


Figure 2.8: Radial MTDC network topology.

2.3.2 Ring Network

This network is perfect where system stability is highly required, but controlling the voltage is very complex. In case of a line outage another path can also be utilized.

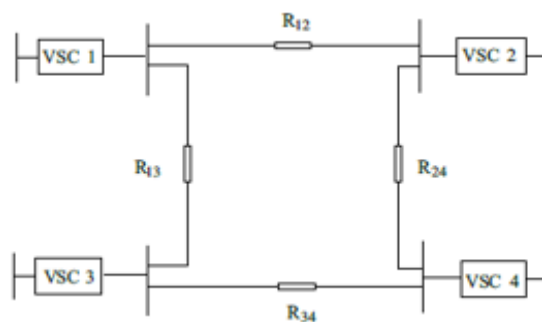


Figure 2.9: Circular MTDC network topology.

2.3.3 Meshed Network

A meshed network is necessity of the future MTDC systems as more and more HVDC links are deployed at different locations with different uses. In a meshed network the DC grid stability and capability to transmit power from different locations is improved [12].

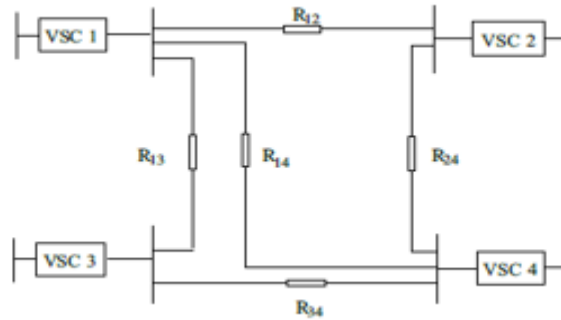


Figure 2.10: Meshed MTDC network topology.

2.4 Line Commutated Converters

2.4.1 Introduction

LCC Type hvdc systems are the most matured and deployed technology among hvdc converter systems due to the simplicity of converter configuration and low cost. For bulk power and very long distance transmission of electrical energy LCC hvdc is the most economical and reliable option in the market today. The Operation of LCC depends upon the line voltage that's why they are called line commutated converters. In LCC two types of semiconductors are used, diodes or thyristors, but due to the advantage of controllability of DC voltage, thyristors are mostly used in traditional HVDC systems.

2.4.2 Thyristors (Operation not included?)

A thyristor is a semiconductor device responsible for providing controlled switching and thus known as the heart of an LCC converter. It is basically a 4-layer combination of p and n type materials with two or three terminals and have the capability of achieving high ratings such as 8500 V, 4500 A. A thyristor is an extended form of a diode with addition of control terminal known as gate as shown in Fig. 2.12.

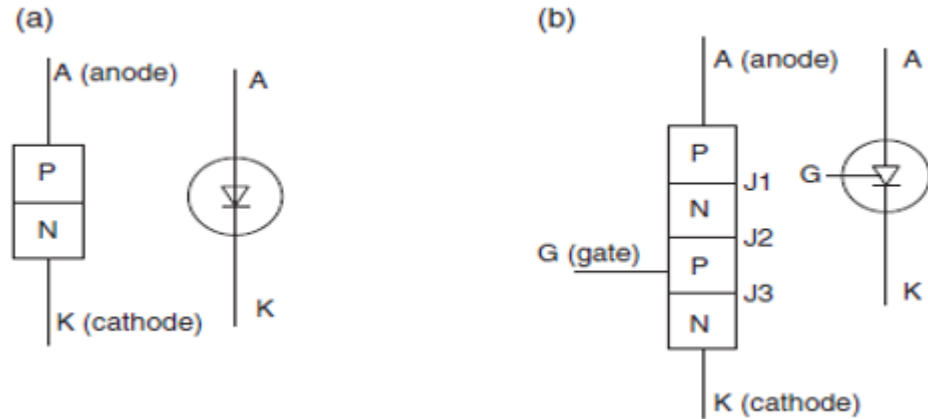


Figure 2.11: Structure and Symbol for (a) diode and (b) thyristor.

2.4.3 Converter Configuration

LCC configurations is based on the basic principles of a simple three phase six or twelve pulse bridge rectifier circuit also known as Graetz Bridge Rectifier as shown in Fig. 2.13. The Circuitry is composed of six controlled electronic switches in pair of two each and every pair connects to the single phase line respectively connecting to two dc terminals.

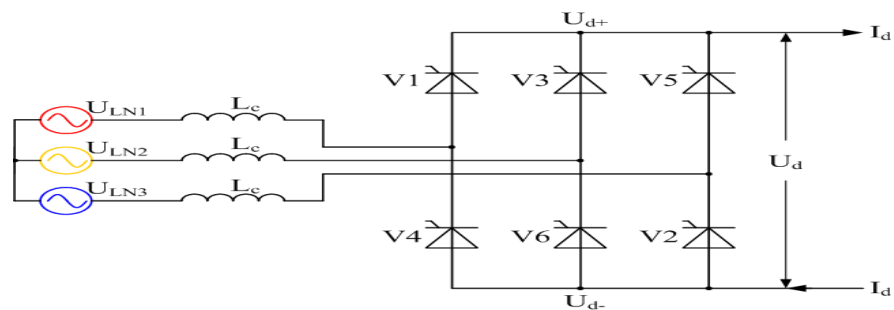


Figure 2.12: Six pulse converter configuration for LCC HVDC.

Two valves connect two ac line voltages to the dc lines as shown in Fig. 2.14. The dc output is taken by the summation of the upper valve voltage minus the lower valve voltage. Due to presence of inductance in the ac mains there is an overlap during the conduction of one pair of valves to the next, for this period the dc output value is taken from average of first pair of valves minus the transitioned valve and so on and this is known as Overlap angle μ . The overlap angle can reach a max of 20° at full load. Due to this μ there is a notch in dc output voltage which decreases mean DC voltage value.

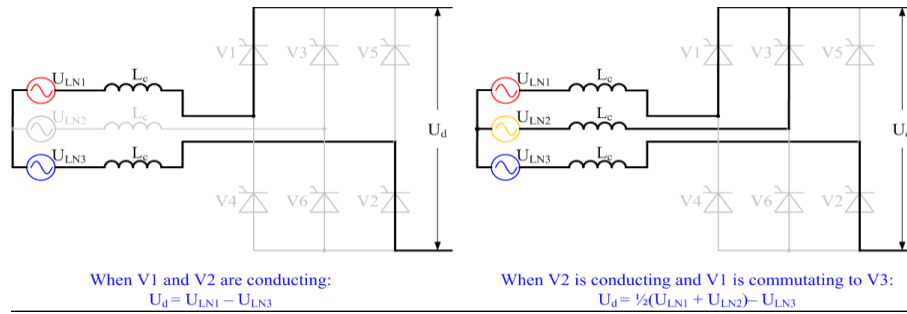


Figure 2.13: Working Principle of Six pulse converter for LCC HVDC.

The average voltage at the output is given by the equation

$$V_{dc} = V_{av} = \frac{3V_{LLpeak}}{\pi} \cos(\alpha) - 6fL_c I_d$$

The Firing angle control is the easiest way to control DC voltage. By increasing the alpha value DC voltage will decrease and vice versa. The rectification and inversion of DC voltage also depends upon alpha value. From angle 0-90° The DC output voltage is positive which corresponds to rectification mode and from 90-180° the dc output voltage becomes negative which corresponds to inversion mode as shown in Fig. 2.15.

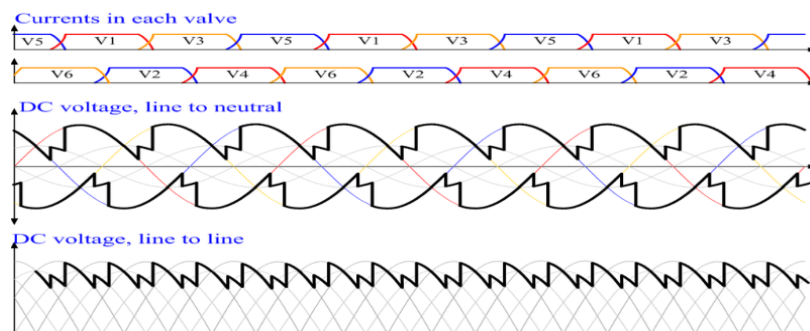


Figure 2.14 Valve waveforms of DC voltages.

Harmonics are introduced in the ac and dc sides of the converter when using a six pulse converter configuration due to change in phase voltages so a 12 Pulse converter configuration based on two six pulse bridges can be seen in Fig. 2.16 is used to reduce these harmonics. This configuration restricts phase change between two ac

supplies to 30° previously 60° which allows the cancellation of voltage and current harmonics.

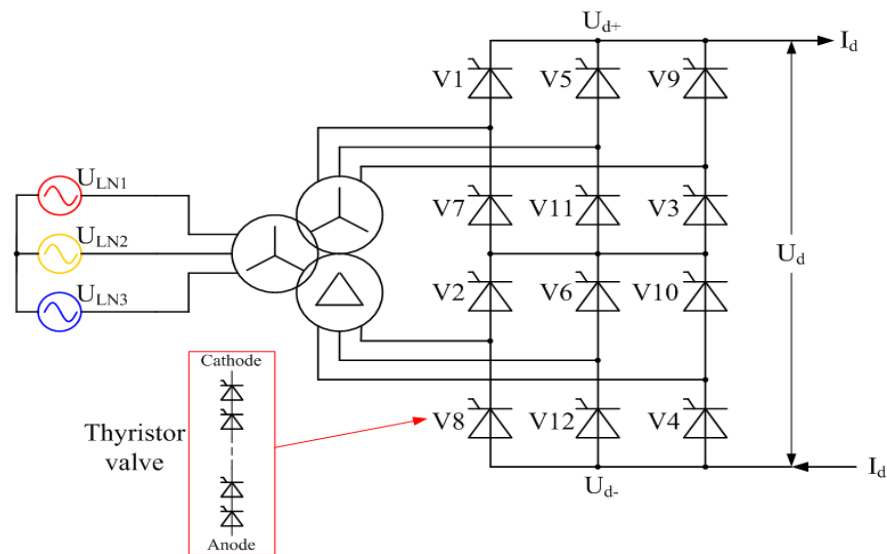


Figure 2.15: Twelve Pulse converter configuration for LCC HVDC.

2.4.4 Advantages and Applications

LCC HVDC is the main used technology for mostly bulk power transfer in long distance transmission systems and will remain there for vast applications as the cost of thyristors is reducing and the rating capabilities are increasing. The two main applications of LCC HVDC systems are Bulk power transfer using point to point systems and submarine transmission systems. Other details of advantages and applications are given in the table.

Table. 2: Advantages and Applications of LCC HVDC system.

S.No	Applications	Configuration Used	Advantages
1	Bulk Power Long Distance Transfer	P2P Links	No reactive power limits
2	Submarine Transmission	B2B Links	Less Cables Required to transfer more power
3	Interconnection between different AC networks with different features	P2P, B2B Links	Interconnecting systems with different frequencies
4	Stabilization of Weak AC grids	P2P, B2B and Multiterminal Links	Fast and Accurate Power Flow Control

2.5 Voltage Source Converters:

2.5.1 Introduction:

The Voltage source converter is based on Insulated gate bipolar transistor (IGBT) type semiconductor technology which has the ability to control both of its turn on and off timings. Simple thyristors restrict the use of LCC type converters against many applications such as feeding power into a passive system, using the converter as a power source in case of islanding, and connecting asynchronous AC grids. The IGBT type converters have many advantages over the thyristor type w.r.t the integration of renewable power sources, the degree of controllability and sustainability of the DC grids. Due to the fixed polarity of DC voltage it can be considered constant which is why these converters are called Voltage source converters. VSC converter technology is a better option for the expansion of a two terminal HVDC into a Multiterminal DC grid which provides the basic infrastructure for the making of supergrids and inter-continental or intra-country grids.

2.5.2 IGBT (Operation Included or not):

It is a semiconductor device made up of four alternating layers of p and n materials and 3 terminals named Gate, Collector and Emitter as shown in Fig. 2.17. It is manufactured by combining the attributes of both MOSFETs and BJTs which give the IGBTs its features of high efficiency and fast switching with low losses. The output characteristics of IGBTs behaves like a BJT whereas input characteristics conducts as MOSFETs thus it works as a Voltage Source device.

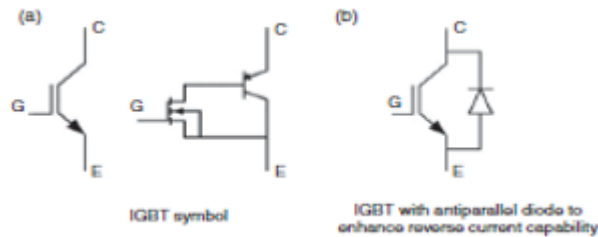


Figure 2.16: Symbol of IGBT circuit.

2.5.3 Two-level converter:

There are basically two types of two level voltage source converters, a single phase two level and a three phase two level VSCs. In recent HVDC systems most of the VSCs are based on three phase two level converters with configuration of a six pulse bridge with IGBTs instead of common thyristors shown in fig 2.18. As the name indicates two level means the output voltage is either a positive or a negative discrete value close to a square wave. When the Upper Valve is conducting the output gives a positive voltage value which is half of the total voltage output ($\frac{1}{2} V$) and similarly happens for the negative half cycle as shown in Fig. 2.19.

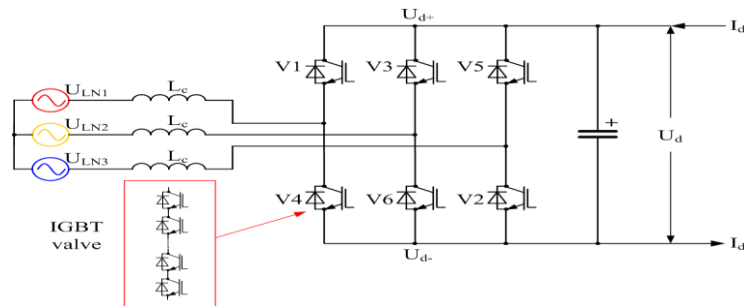


Figure 2.17: Two level Six pulse VSC HvdC converter configuration.

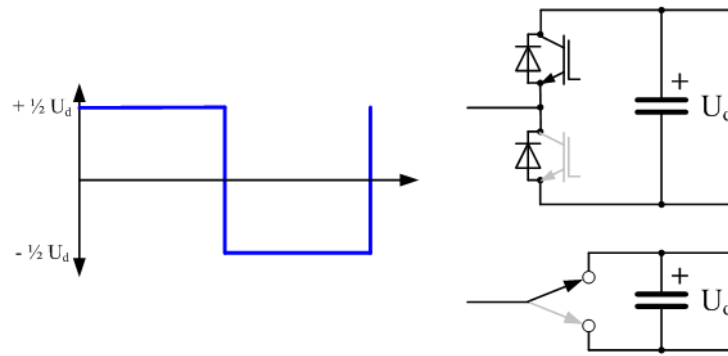


Figure 2.18: Internal valve circuitry (Too and fro switch).

The main drawback of this configuration is that the output wave is very inefficient as there are huge harmonic distortions and requires PWM techniques to overcome this problem. The overall efficiency is reduced with the use of PWM as the IGBTs have to turn off and on too many times. The overall efficiency of two level VSC is less than an LCC and to improve that hundreds of IGBTs are required to be connected in series in each valve, which obviously will increase the overall losses and costs. For such reasons three level and Multilevel converter configurations are introduced.

2.5.4 Three Level Converter:

To overcome the disadvantages of two level converters these converters introduced another discrete value of “0” with “ $\pm 1/2 V$ ” by adding another IGBT valve with all six valves. Such a configuration is known as Neutral Point clamped or diode clamped converter. It works as a single pole triple throw switch as shown in the fig. Each Phase contains four valves. Two series diodes are connected parallel to each of the second and third IGBT valve in every phase. These diodes are then connected to the midpoint of two series capacitors connected parallel to the arms of the converter as shown in the Fig. 2.20.

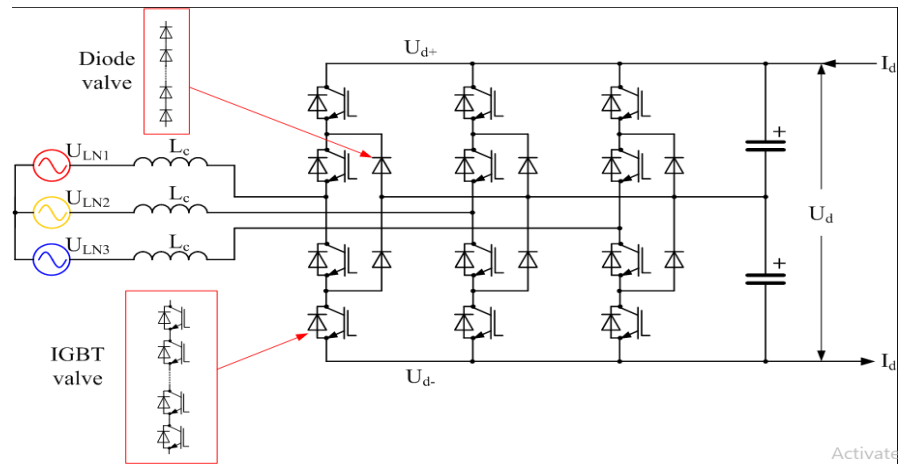


Figure 2.19: Three Level VSC HVDC converter configuration with antiparallel diodes.

The Positive output value is achieved by turning the first two IGBT Valves whereas the negative output value is achieved by turning the last two IGBT valves and the zero output value is achieved by turning the middle two valves on as shown in the Fig. 2.21. The parallel diodes (clamping diodes) provides the current path through the phases simultaneously.

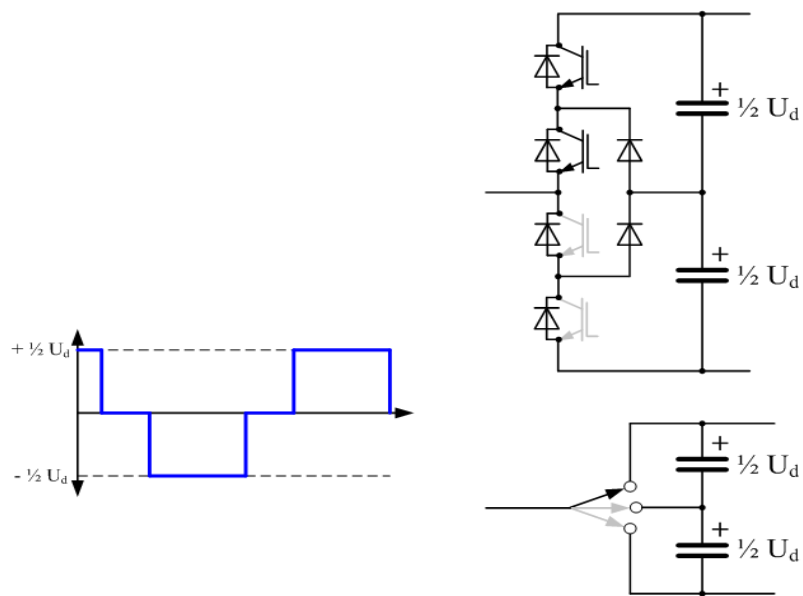


Figure 2.21: Waveform generation from single arm circuit of three level VSC converter.

2.6 Modular Multilevel Converters:

Multilevel converter technology is considered the most viable option for the expansion of current HVDC links into Multiterminal grids. The drawbacks of using two level converters can be easily overcome by increasing the number of IGBTs in series in a valve and pairing up these IGBTs to form submodules, this also proves to be an effective way of overcoming dc faults due to the independent control provided for the individual submodule with its storage capacitor. A two level converter generates only two discrete output voltage values as shown in Fig. 2.22 a. A three level converter generated three discrete output voltage values as shown in Fig. 2.22 b and a five level converter generates five voltage values as shown in Fig. 2.22 c. Similarly by increasing the switching levels the output voltage will be nearly like AC sinusoidal with reduced THD harmonics.

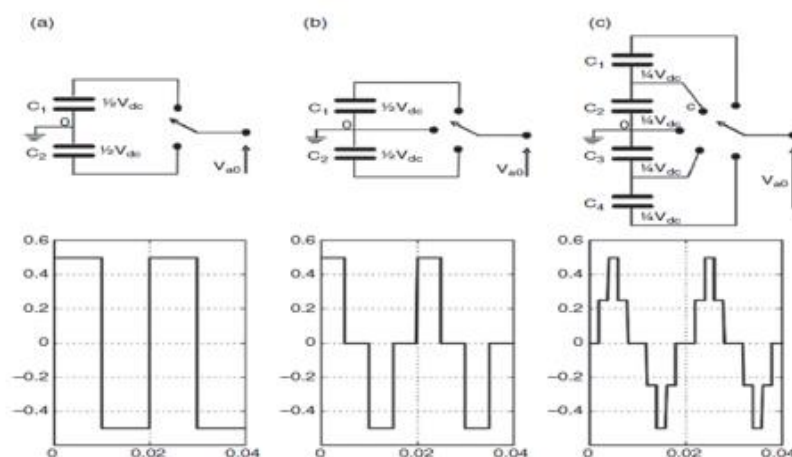


Figure 2.20: One Phase leg of VSC HVDC converter with (a) two levels, (b) three levels, (c) five levels.

Each submodule is composed of either a half bridge or a full bridge converter. The N submodules are connected in series to form an arm and two arms are connected in series through Inductors to limit fault currents and also control the circulating currents as shown in Fig. In an MMC currents goes directly in all six valves unlike in an LCC. Therefore the valve current only depends upon direct current which split in three phases and alternating currents which splits in the upper and lower arms.

2.6.1 Module Topologies:

There are different submodule topologies available for different applications of the MMC converters. The most common module topologies are half bridge and full bridge topologies. The half bridge topology is composed of two IGBTs, two parallel diodes and one capacitor connected in parallel with both IGBTs whereas a full bridge topology comprises of four IGBTs, four diodes and one capacitor giving an extra advantage of fault clearing capability.

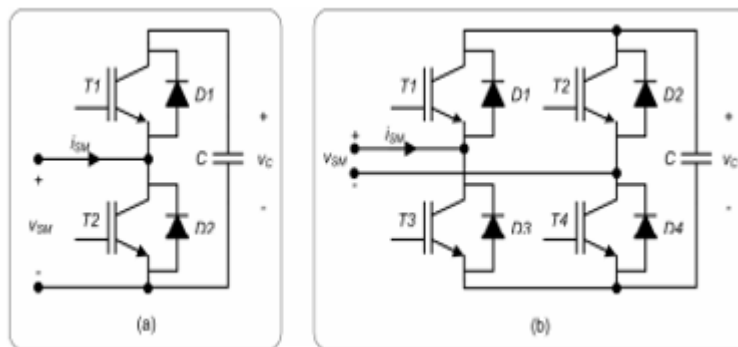


Figure 2.21: Switching module (SM) topologies: (a) half bridge; (b) full bridge.

2.7 Hybrid Converters:

For attaining the benefits from the above discussed types of converters a hybrid converter can be designed from any of the converter configuration for a specific scenario to achieve the ultimate goal of a more reliable and flexible DC grid. However designing such a converter requires state of art research. The main advantages include huge cost reductions and low footprint. Till date there are three types of possible converter topologies. A hybrid three terminal HVDC shown in Fig. 2.25 provides integration of AC system with VSC and LCC stations located at different places. This type of topology provides the basics for the expansion of three terminal systems into Multiterminal HVDC systems. Some other advantages include high quality energy transmission to remote area load centers and islands. [13]

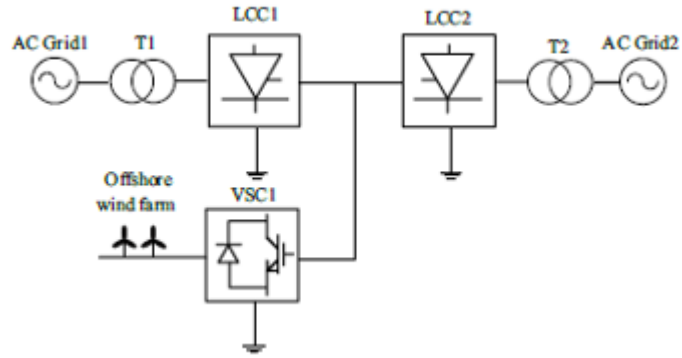


Figure 2.22: Three terminal Hybrid HVDC transmission system.

Another type of hybrid converter topology shown in Fig. 2.26 is the Hybrid bipolar HVDC system where both type of converters are connected at different poles of a same station. By utilizing the advantage of VSC's reactive power control capabilities, the use of ac filters can be avoided saving costs and low footprints at the station. This topology is also helpful for connecting weak AC grids.

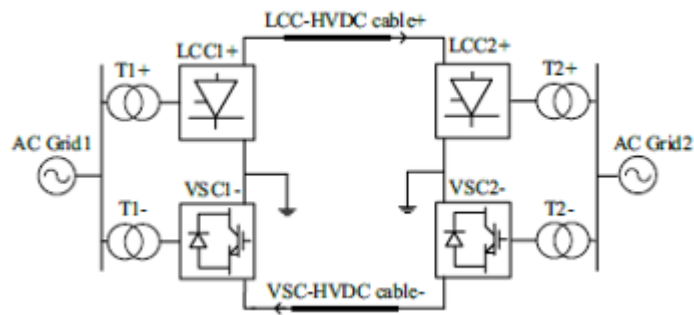


Figure 2.23: Four-terminal Bipolar Hybrid HVDC transmission system.

A multi-infeed system is consisted of different topological interconnections of LCC and VSC HVDC systems connected through a single AC bus system as shown in Fig. 2.27. One of the main advantage of this configuration is the use of effective control of reactive power requirements during commutation failures to keep the passive network stable.

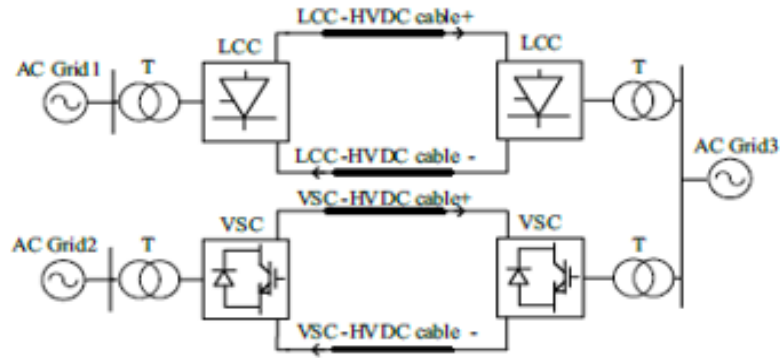


Figure 2.24: Dual-infeed Hybrid dual-infeed HVDC transmission system.

2.8 DC to DC Converters in HVDC

The DC to DC converters used specifically for HVDC application are classified into two main classes which are further divided into multiple subclasses depending on their application as shown in Fig. 2.28 [14]

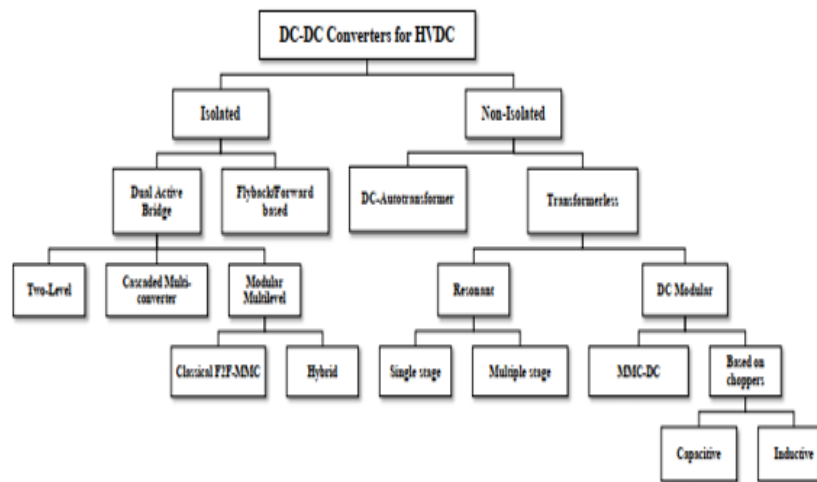


Figure 2.25: DC-DC Proposed classification for HVDC converters application flow chart.

2.9 Abnormal Conditions

The two main abnormal conditions in HVDC grids include AC voltage sags and DC voltage sags which creates stresses on the system and distorts the system behavior. AC voltage sags are further divided into three categories.

1. One phase to ground fault or 30% sag in the ac side voltage.
2. Two phase to ground fault or 70% sag in the ac side voltage.
3. Three phase to ground fault or 100% sag in the ac side voltage.

References

- [12] Gowaid IA, Page F, Adam GP et al (2015) Ring DC node configurations for enhanced DC fault protection in multiterminal HVDC networks. International Conference on Renewable Energy Research and Applications (ICRERA), Palermo, Italy, 22-25 Nov. 2015, 5p
- [13] Torres-Olguin RE, Molinas M, Undeland T (2012) Offshore wind farm grid integration by VSC technology with LCC-based HVDC transmission. IEEE Transactions on Sustainable Energy, 3(4):899-907
- [14] R. Zeng, L. Xu and L. Yao, "DC/DC Converters Based on Hybrid MMC for HVDC Grid Interconnection," 11th IET International Conference on AC and DC Power Transmission, Birmingham, pp. 1-6, 2015

Chapter 3: Modeling Control and Operation of HVDC Converters

3.1 Modeling Control and Operation of LCC HVDC grids

3.1.1 Operational Characteristics of LCC HVDC

A two terminal model is shown in Fig. 3.1 (a). $V_{dor}\cos\alpha$ represents the rectifier voltage whereas $V_{doi}\cos\gamma$ represents the inverter voltage in Fig.3.1 (b). It is assumed that the current is flowing from rectifier to inverter. Line resistance, rectifier circuit resistance and inverter circuit resistances are also taken into the account. Hence the total current I_d is alpha and gamma provides the basic control mechanism for the LCC HVDC.

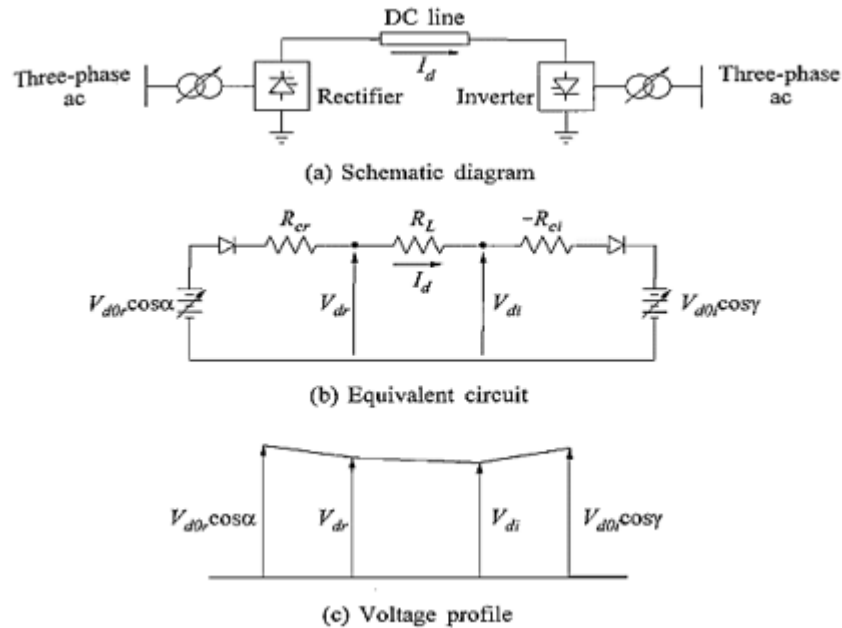


Figure 3.1: HVDC Transmission link (a) schematic diagram, (b) equivalent circuit, (c) voltage profile.

$$I_d = \frac{V_{dor}\cos\alpha - V_{doi}\cos\gamma}{R_{cr} + R_L - R_{ci}}$$

The control characteristic curves provided in Fig. 3.4 represents the control modes available for the LCC HVDC under normal or faulty conditions. The basic

means of controls can be achieved through managing the internal voltages; $V_{dor}\cos\alpha$ and $V_{doi}\cos\gamma$ as controlling the firing angles will eventually help in increasing or decreasing the DC currents.

3.1.2 Ideal Steady State Characteristics:

Both the stations are assigned different control options. During normal operation rectifier is assigned with Constant current mode and inverter is at constant extinction angle control. DC voltage is measured at rectifier. Curve AB comprises of CIA (constant ignition angle) control mode where alpha is rated at a minimum angle of 5 for forcing current to stay under rated value. The curve BY comprises of CC (constant current) mode. It is set according to the desired reference value and after a complete reversal of voltage after 90 degrees the characteristics are changed to the inverter mode. The curve XY comprises of CEA (constant extinction angle control) which is also kept at a minimum angle of 10.

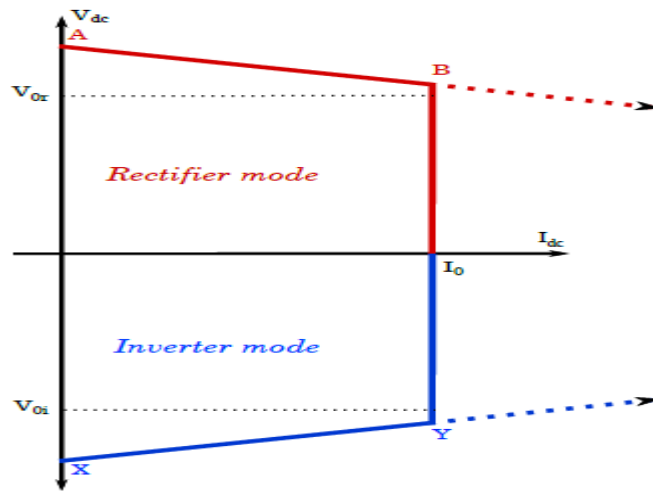


Figure 3.2: Ideal steady state characteristics.

By applying rectifier and inverter characteristics on the same plot basic operational points can be achieved. To obtain a basic operating point OP1, first the current order is determined using an outer power loop for the rectifier. This will allow the inverter to obtain its current order by subtracting from Margin current. In case of an AC voltage sag at the rectifier, the DC voltage reduces forcing the operating point to go from OP1 to Op1` and further reduction in DC voltage due to any other cause

will make OP2 the new operating point. Here Inverter controls the DC current and rectifier switches to CIA mode.

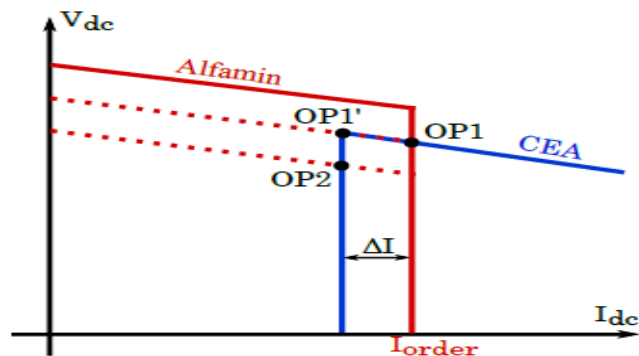


Figure 3.3: Alpha and gamma characteristics based rectifier and inverter modes.

3.1.3 Actual Steady state Characteristics and Basic Control Strategies of LCC

The basic purpose here is to find the optimal operating point depending on the practical system requirements. Under normal operating conditions, the inverter controls the DC voltage whereas the rectifier is assigned to control the DC current. Points ABCD shows the minimum extinction angle characteristics where either “g” is maintained at a constant value and DC voltage droop is dependent on increasing or decreasing currents. Likewise DC voltage can be kept constant using points BHE so that CEA “g” is used to handle increasing or decreasing currents.

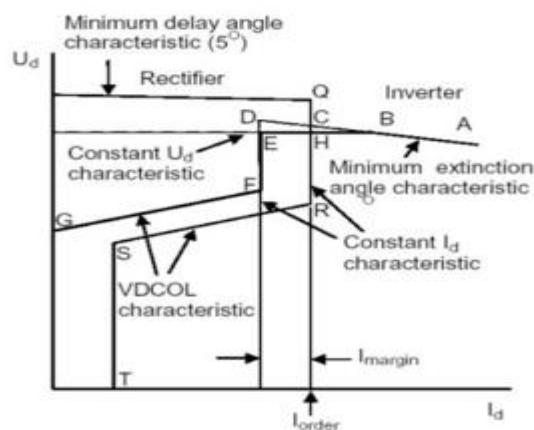


Figure 3.4: Actual steady state characteristics of voltage and current for a two terminal LCC HVDC system.

Rectifier is assigned to control the DC current so points QCHR correspond to steady state characteristics of current control mode of the rectifier controls. The controller then decides to points C or H as intersecting points of rectifier and inverter characteristics according to the design requirements. If the I_{order} current of the rectifier is increased beyond point B, the inverter in case of constant DC voltage control mode starts operating in CEA control mode with characteristic curve of AB.

If I_{order} current cannot be maintained and falls below a certain value till I_{margin} is sustained then the rectifier is assigned to control the DC voltage with characteristic PQ and inverter is assigned automatically to control DC current with characteristics DEF.

Further drop in the DC voltage can be hazardous with this control mode. For this reason voltage dependent current order limiter (VDCOL) controller is used to maintain the I_{order} current to a minimum using rectifier characteristics RST and inverter characteristics FG till the system is recovered.

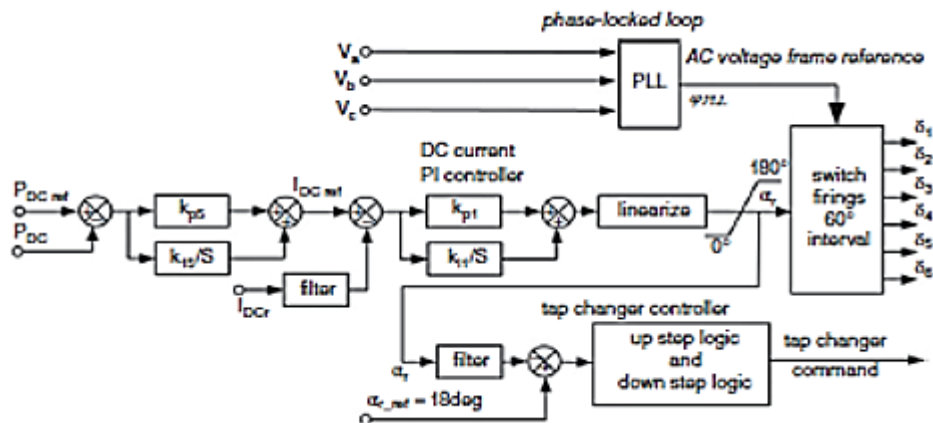


Figure 3.5: Rectifier and Inverter Controller schematics.

3.2 Modeling Control and Operation of VSC HVDC grids

3.2.1 Modeling of VSC Station

A single phase diagram of VSC is assumed as an average value model to simplify and acquire the modeling for VSC control system. A phase reactor L_r connects the ideal voltage source (AC side) of the VSC to the point of common coupling. Whereas the dc side of VSC is considered as a current source connected to V_{dc} with 2 parallel capacitors.

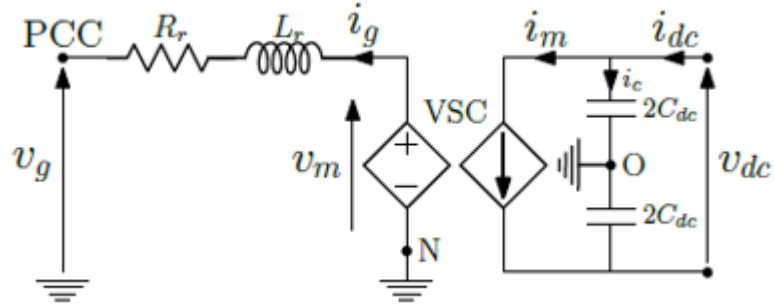


Figure 3.6: One phase schematic diagram of VSC two terminal HVDC link

First the equations for AC side of the VSC are derived by applying KVL for each phase j we get eq. 3.1. D-axis and Q-axis equations are transformed for simplicity from this three phase equation 3.1, whereas ω_g represents the grid ac frequency.

$$v_{m,j}(t) - v_{g,j}(t) = L_r \frac{di_{g,j}(t)}{dt} + R_r i_{g,j}(t) \quad (3.1)$$

$$v_{m,d} - v_{g,d} = L_r \frac{di_{g,d}}{dt} + R_r i_{g,d} - \omega_g L_r i_{g,q} \quad (3.2)$$

$$v_{m,q} - v_{g,q} = L_r \frac{di_{g,q}}{dt} + R_r i_{g,q} + \omega_g L_r i_{g,d} \quad (3.3)$$

Similarly for the dc side as it is connected to a current source the DC current is;

$$i_c = i_{dc} - i_m = C_{dc} \frac{dv_{dc}}{dt} \quad (3.4)$$

As the losses are neglected the ac active power can be considered to be equal to dc power as shown in equation. Also from this equation i_m can be derived as equation 3.6.

$$p_{ac} = v_{m,d}i_{g,d} + v_{m,q}i_{g,q} = v_{dc}i_m = p_{dc} \quad (3.5)$$

$$i_m = m_d i_{g,d} + m_q i_{g,q} \quad (3.6)$$

Complete model of Ac and DC sides can be made from the above equations by applying Laplace transformation.

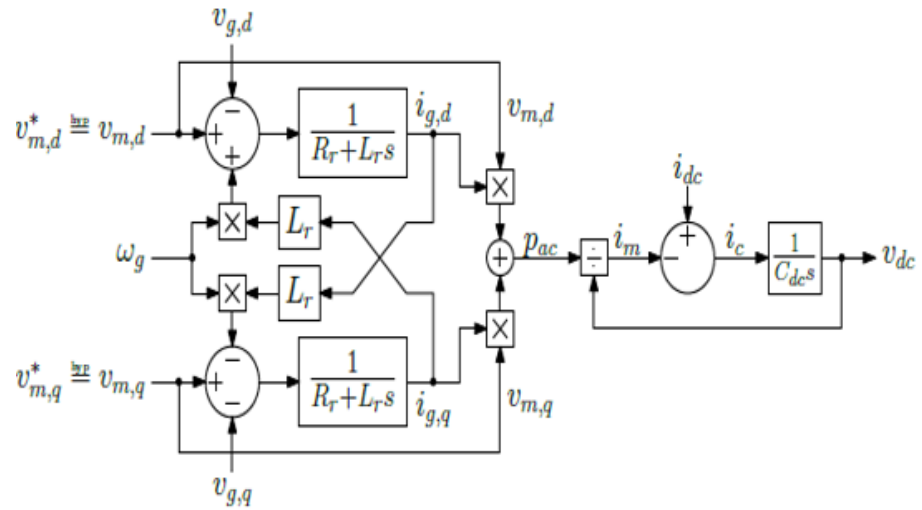


Figure 3.7: AC and DC side Modelling of VSC system.

3.2.2 Control of VSC station:

The Control of VSC is divided into mainly two loops, an inner current loop and an outer voltage or power loop thus providing independent active and reactive power control with the help of PWM technology. The Complete block diagram of the novel control strategy of grid connected VSC station is shown in Fig. 3.8 the active and reactive powers are controlled by the magnitude and angle of the ac side equivalent voltage V_m of the VSC. Clarks transformation is used to convert three phase voltages and currents from the ac grid into two phase dq transformations whereas angle

(theta) is determined using phase locked loop (PLL) to further feed the PWM with three phase synchronized values. The Inner and Outer control loops are described in detail below.

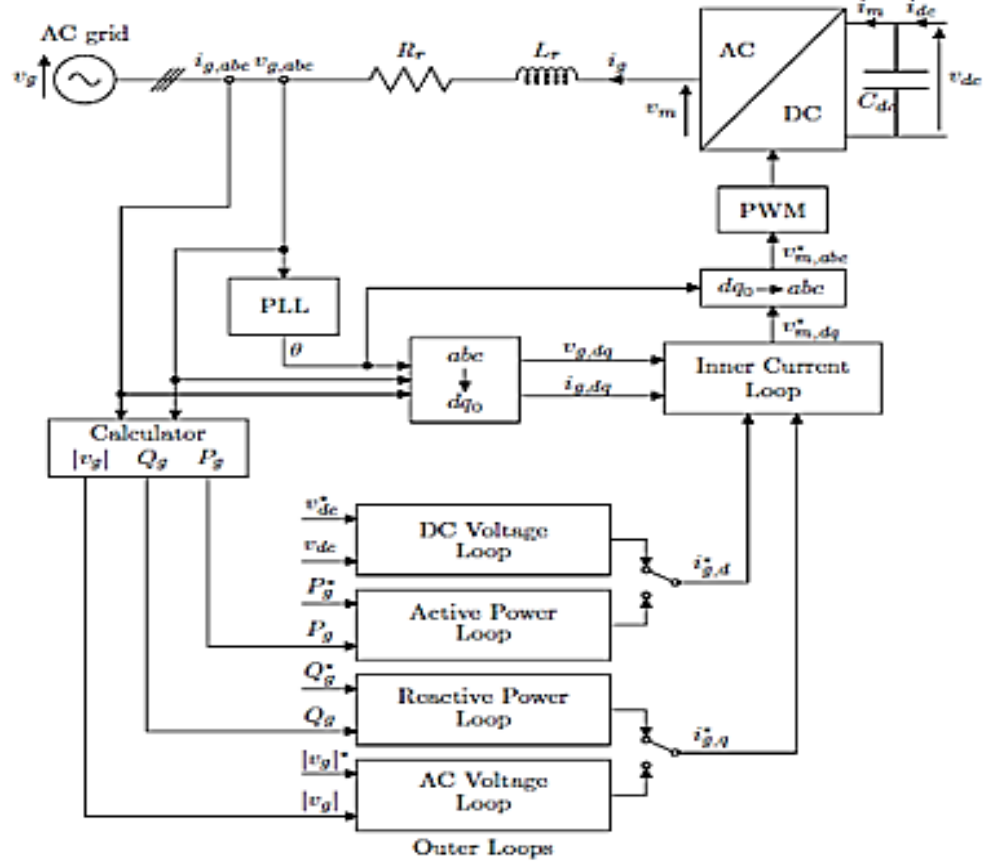


Figure 3.8: Complete control strategy for VSC HVDC system.

3.2.3 Inner Vector Current control Loop:

A vector inner control loop is also known as the current control loop as it uses the differential decoupling DQ reference currents to independently control both the active and reactive powers.

$$v_{m,d}^* = C(s) (i_{g,d}^* - i_{g,d}) + v_{g,d} - \omega_{PLL} L_r i_{g,q} \quad (3.7)$$

$$v_{m,q}^* = C(s) (i_{g,q}^* - i_{g,q}) + v_{g,q} + \omega_{PLL} L_r i_{g,d} \quad (3.8)$$

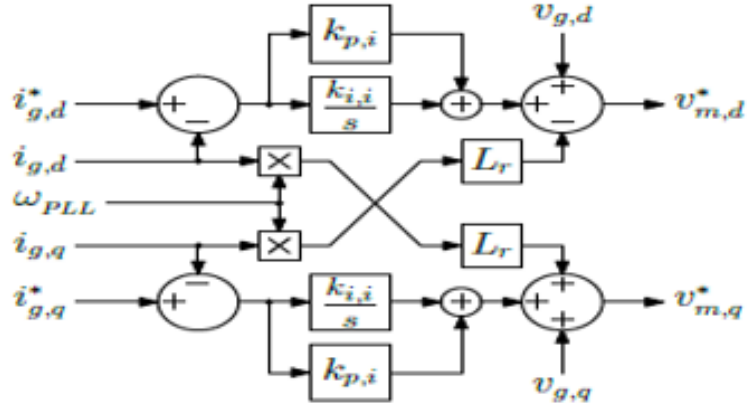


Figure 3.9: Inner control loop modeling of VSC converter.

3.2.4 Outer Control Loop:

Outer control loops includes the AC and DC voltages or active or reactive power controls. Outer control loop also provides the d and q-axis reference currents $I_{g,d}^*$ and $I_{g,q}^*$ for decoupling with the inner vector current loop as active power and reactive power solely can be controlled using d-axis and q-axis of the dq0 reference frame since d-axis is lined up with phase a and q-axis is lined up with phase b of the grid voltages. The active and reactive power equations at point of common coupling are shown in equations 3.9 and 3.10. The reference currents of d-axis and q-axis are then generated as shown in equation 3.11 and 3.12 for inner current control loops, which can be then Laplace transformed as shown in Fig. 3.10.

$$P_g = v_{g,d} i_{g,d} \quad (3.9)$$

$$Q_g = v_{g,d} i_{g,q} \quad (3.10)$$

$$i_{g,d}^* = \frac{P_g^*}{v_{g,d}} \quad (3.11)$$

$$i_{g,q}^* = \frac{P_g^*}{v_{g,q}} \quad (3.12)$$

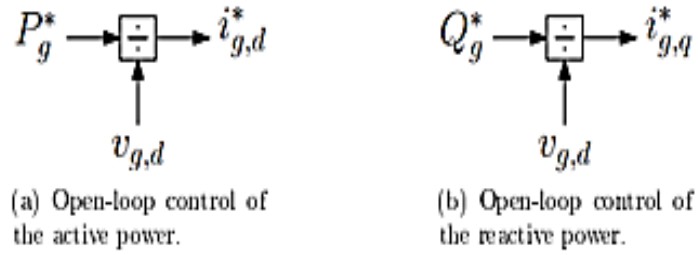


Figure 3.10: Open loop control of (a) active and (b) reactive power controllers.

Instead of generating d-axis and q-axis reference currents from active and reactive powers, an AC voltage or DC voltage controllers can do the same. By increasing or decreasing power through regulating the d-axis current, the DC voltage controller is used to control the DC voltage level on the dc side similarly the q-axis current can be regulated to control the PCC voltage with the help of AC voltage controller. The Complete Control model is shown in fig with all four outer control loops and inner control loop. All inner and outer control loops uses PI controllers for optimal control of the system.

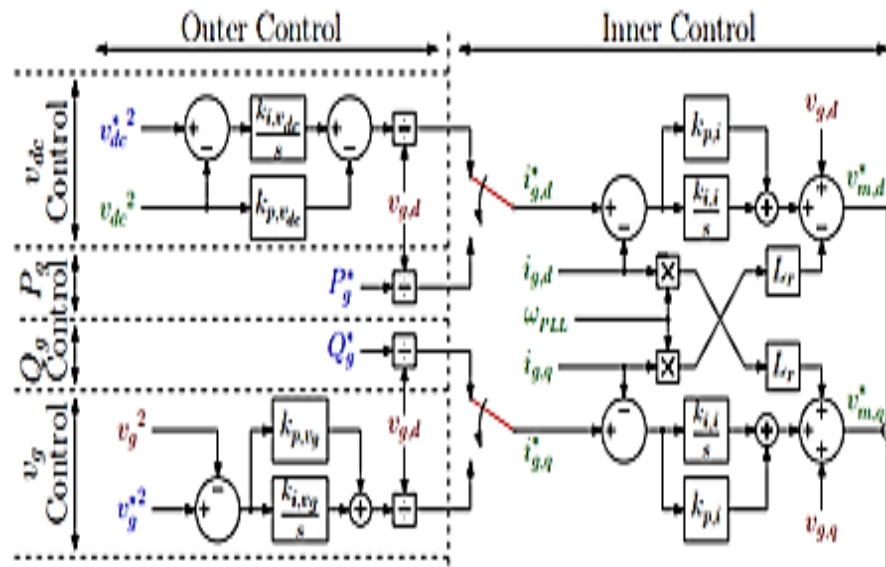


Figure 3.11: Modeling of complete control system of inner and outer controls.

3.3 Modeling Control and Operation of MMC HVDC grids

3.3.1 Modeling of MMC station

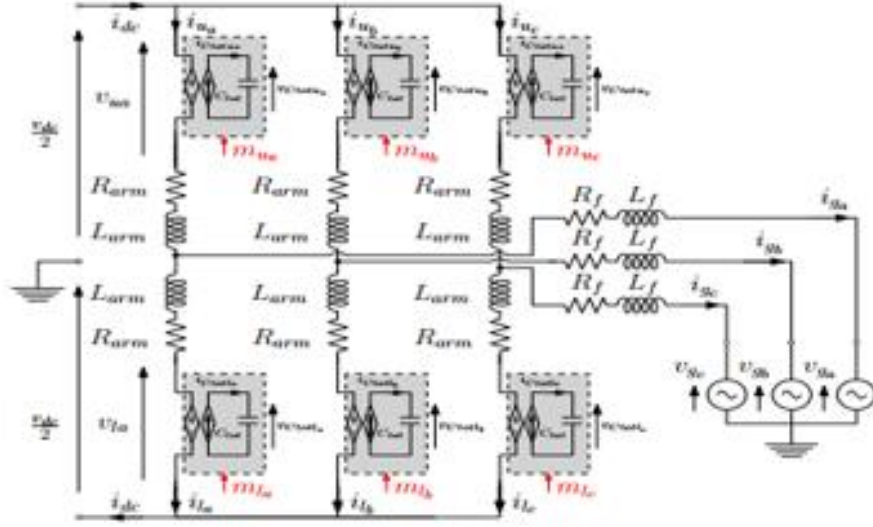


Figure 3.12: Representation of detailed Arm Average Model of a MMC converter.

$$v_{uj} = m_{uj}v_{Ctotuj} \quad v_{lj} = m_{lj}v_{Ctotlj} \quad (3.13)$$

$$i_{Ctotuj} = m_{uj}i_{uj} \quad i_{Ctotlj} = m_{lj}i_{lj} \quad (3.14)$$

$$\frac{v_{dc}}{2} - v_{uj} - L_{arm} \frac{di_{uj}}{dt} - R_{arm}i_{uj} - L_f \frac{di_{gj}}{dt} - R_f i_{gj} - v_{gj} = 0 \quad (3.15)$$

$$\frac{-v_{dc}}{2} + v_{lj} + L_{arm} \frac{di_{lj}}{dt} + R_{arm}i_{lj} - L_f \frac{di_{gj}}{dt} - R_f i_{gj} - v_{gj} = 0 \quad (3.16)$$

$$v_{mj} - v_{gj} = L_{eq}^{ac} \frac{di_{gj}}{dt} + R_{eq}^{ac} i_{gj} \quad (3.17)$$

$$v_{dc} - v_{diffj} = 2L_{arm} \frac{di_{diffj}}{dt} + 2R_{arm}i_{diffj} \quad (3.18)$$

$$v_{Ctotuj} = v_{Ctotlj} = \bar{v}_{Ctotj} \quad (3.19)$$

$$2C_{tot} \frac{d\bar{v}_{Ctotj}}{dt} = m_{uj}i_{uj} + m_{lj}i_{lj} \quad (3.20)$$

$$2C_{tot} \frac{d\bar{v}_{Ctotj}}{dt} = m_{acj}i_{diffj} - m_{acj}i_{gj} = i_{mdcj} - i_{macj} \quad (3.21)$$

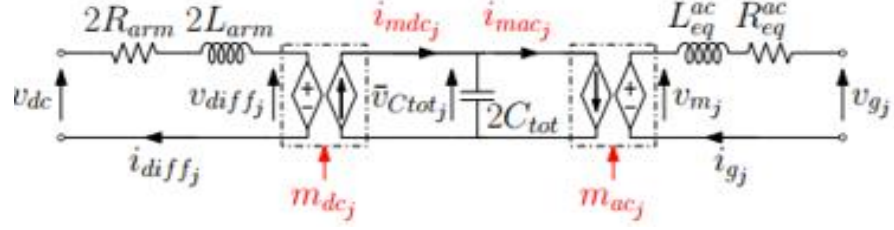


Figure 3.13: Equivalent circuit of each AAM phase.

$$\bar{v}_{Ctot a} = \bar{v}_{Ctot b} = \bar{v}_{Ctot c} = \bar{v}_{Ctot} \quad (3.22)$$

$$C_{eq} \frac{d\bar{v}_{Ctot}}{dt} = \sum_{j=a,b,c} i_{mdc_j} - \sum_{j=a,b,c} i_{mac_j} \quad (3.23)$$

$$P_{mac} = v_{m,d} i_{g,d} + v_{m,q} i_{g,q} = (m_d i_{g,d} + m_q i_{g,q}) \bar{v}_{Ctot} \quad (3.24)$$

$$C_{eq} \frac{d\bar{v}_{Ctot}}{dt} = m_{dc} i_{dc} - m_d i_{g,d} - m_q i_{g,q} \quad (3.25)$$

$$v_{m,d} - v_{g,d} = L_{eq}^{ac} \frac{di_{g,d}}{dt} + R_{eq}^{ac} i_{g,d} - \omega_g L_{eq}^{ac} i_{g,q} \quad (3.26)$$

$$v_{m,q} - v_{g,q} = L_{eq}^{ac} \frac{di_{g,q}}{dt} + R_{eq}^{ac} i_{g,q} + \omega_g L_{eq}^{ac} i_{g,d} \quad (3.26)$$

$$v_{dc} - v_{mdc} = L_{eq}^{dc} \frac{di_{dc}}{dt} + R_{eq}^{dc} i_{dc} \quad (3.27)$$

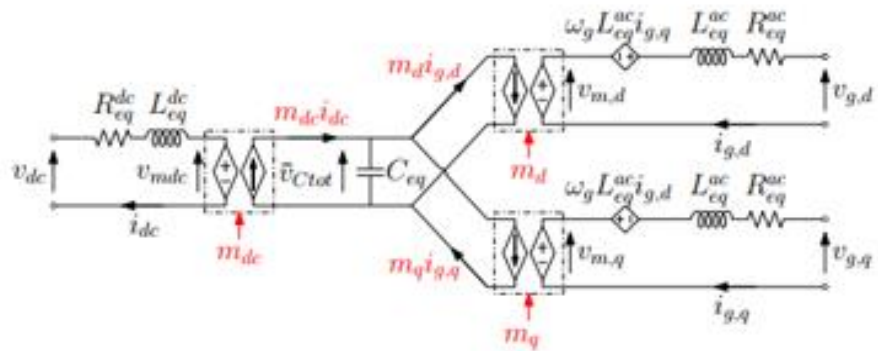


Figure 3.14: Simplified MMC model circuit in dq0 reference frame.

$$C_{eq} \bar{v}_{ctot} \frac{d\bar{v}_{ctot}}{dt} = m_{dc} i_{dc} \bar{v}_{ctot} - v_{m,d} i_{g,d} - v_{m,q} i_{g,q} \quad (3.28)$$

$$\frac{dW_{tot}}{dt} = v_{m,dc} i_{dc} - (v_{m,d} i_{g,d} + v_{m,q} i_{g,q}) = P_{dc} - P_{ac} \quad (3.29)$$

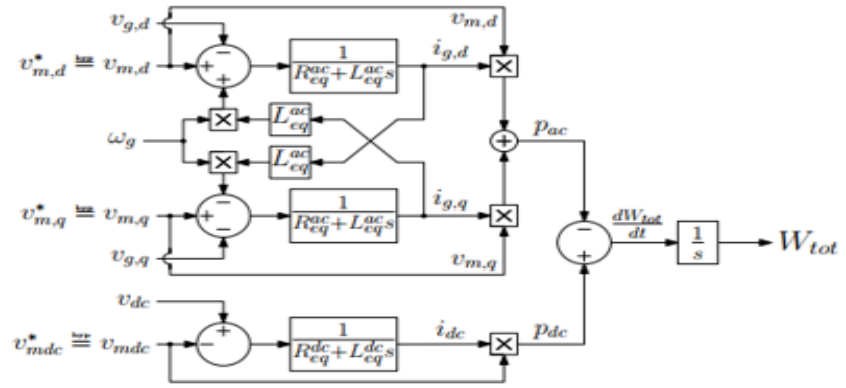


Figure 3.15: Block diagram modeling of complete MMC physical system.

3.3.2 Control Structure of MMC station

3.3.2.1 Inner Control Loop

$$v_{m,dc}^* = v_{dc} - C(s)(i_{dc}^* - i_{dc}) \quad (3.30)$$

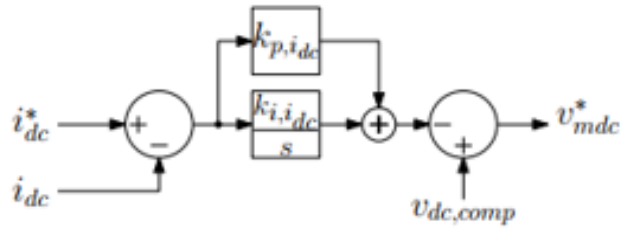


Figure 3.16: DC current loop modelling of MMC converter.

3.3.2.2 Outer Control Loop

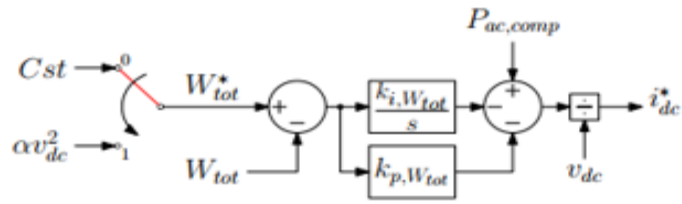


Figure 3.17: Total energy control modelling of MMC converter.

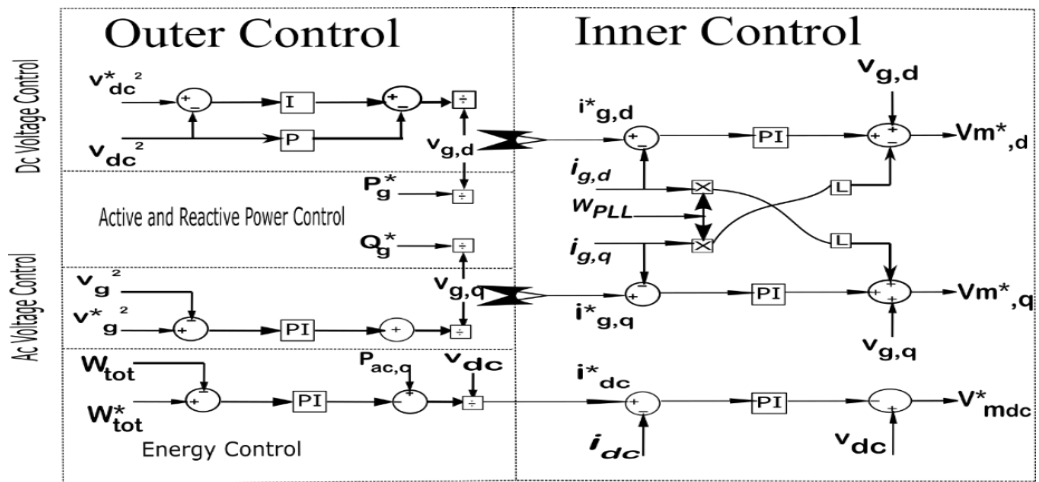


Figure 3.18: Complete physical model of outer and inner control of MMC converter.

Chapter 4: Proposed Case study for Hybrid MTDC Grid

The Fig.4.1 presents the block diagram of this proposed Hybrid MTDC grid system. A Five-Terminal Hybrid MTDC grid is considered, which is integrating multiple AC sources using two different types of HVDC converter technologies. A DC system and a remote area load are further integrated to accurately estimate and depict the performance of this configuration for future complex case studies. Depending upon the nature of control systems of the converters, this grid system is hence subdivided into network zones as shown in Fig. 4.2. These zones are inter-linked with each other using DC-DC converters.

The 12-pulse Line commutated converters are supporting a peak transfer of 500MW power from AC system 1 to AC system 2, which is also shown in a separate block as network zone 1 in Fig.4.2. Both converters are constructed on CIGRE benchmark models [15], [16]. The two LCC systems are transmitting power radially from converter LCC1 to converter LCC2. Three Multilevel Modular Converters (B3, F1, and E1) are connected together in a series interconnection with half bridge converter configuration and are shown in a separate block shown as network zone 2 in Fig.4.2. MMC converter F1 is the offshore inverter and transmitting power from Strong AC system 4 to a strong AC system 3 and also an offshore area Load via converters B3 and E1. DC sources are also considered and is shown as a 3rd network zone in Fig.4.2, transmitting DC power directly to network zone 2 using DC-DC converter. To improve the behavior of the dc voltage under abnormal conditions, two main objectives are considered; improving the fault management capabilities and to lessen the dependency on mechanical circuit breakers. For these objectives the above discussed network zones are inter-connected to each other using DC-DC converters and tested under different topological configurations. One 400kv-400kv DC-DC converter 1 is used to connect network zone 1 and 2 as shown in Fig.4.2 and another adjustable DC-DC converter 2 is connecting network zone 2 and 3. This forms a meshed type HVDC grid with Hybrid Multi-terminal Configuration system. The data used in the models is available in table 4.

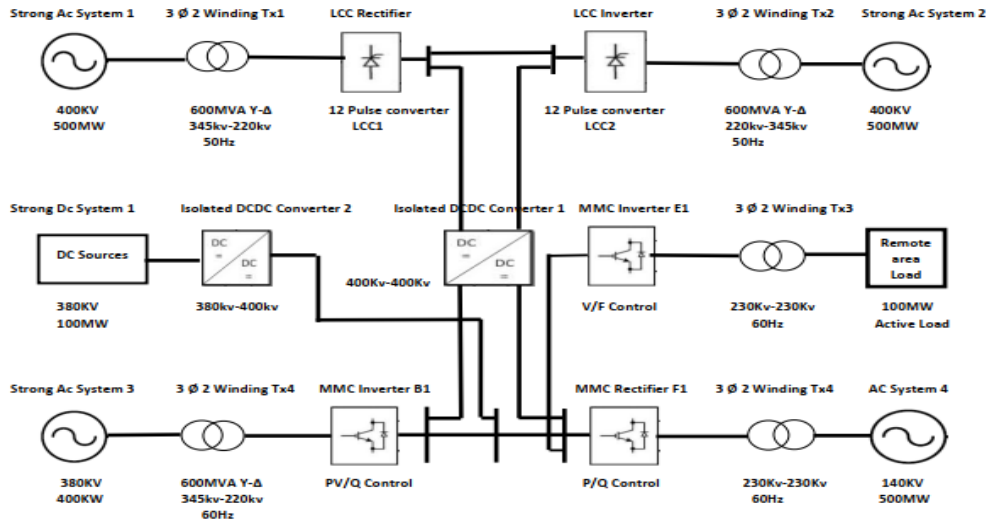


Figure 4.1: Proposed seven terminal MTDC Hybrid LCC-MMC HVDC Circuit Model.

Table. 3: System Data for AC and DC grids and Converters.

AC/DC System	Voltage [KV]	Type	Connected By
AC System 1	400	Onshore Coal	LCC Rectifier
AC System 2	250	Onshore AC System	LCC Inverter
AC System 3	380	Onshore AC System	MMC Inverter (B1)
AC System 4	145	Offshore Wind	MMC Rectifier (F1)
DC System 1	380	PV/battery	DCDC2
AC Load 1	145	Active	MMC inverter (E1)

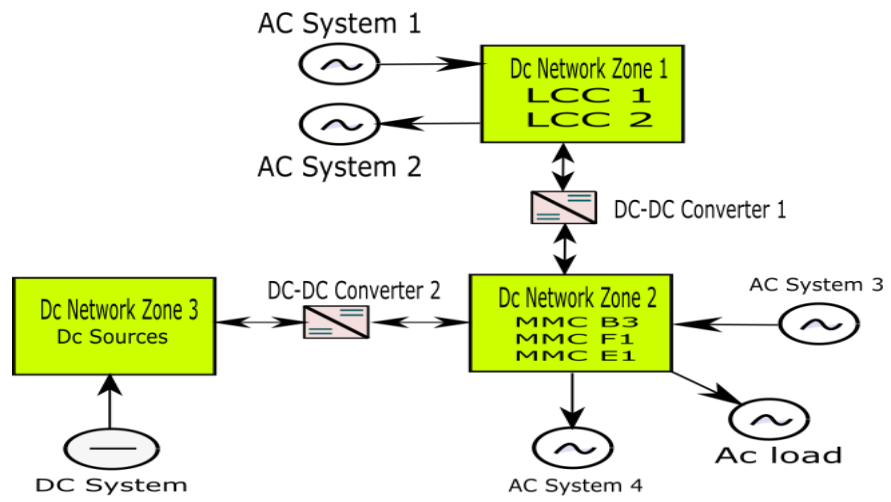


Figure 4.2: HVDC networks divided into network zones on the basis of HVDC grid types.

References

- [14] INTERNATIONAL CONFERENCE ON AC AND DC POWER TRANSMISSION, BIRMINGHAM, PP. 1-6, 2015.
- [15] CIGRE TB 604, Guide for the Development of Models for HVDC converters in a HVDC Grid, CIGRE WG B4-57, December 2014.
- [16] Manitoba HVDC Research Centre, "MyCentre," 10 08 2016. [Online]. Available: [https://hvdc.ca/knowledge base/read, article/57/cigre-b4-57-working-group-developed-models/v](https://hvdc.ca/knowledge_base/read_article/57/cigre-b4-57-working-group-developed-models/v).

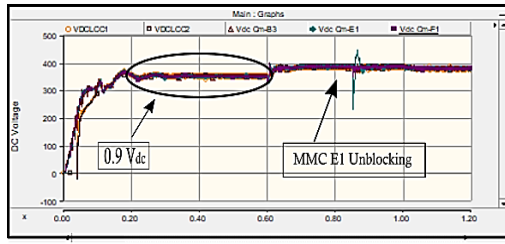
Chapter 5: Results and Analysis

5.1 Grid Start-Up Schemes

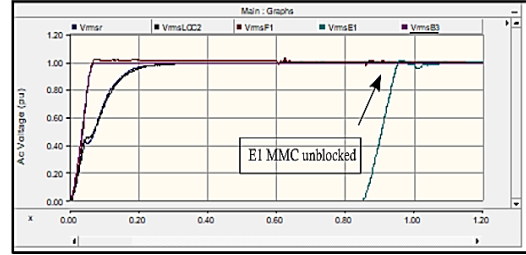
In the start the system needs a withholding current as the DC voltage of the grid is null. This value is provided from the first network zone's LCC inverters. To energize the whole hybrid grid at least one network zone should be capable of providing the initial currents, therefore in this case multi modular converters in network zone two are kept in a blocked state initially and network zone one is unblocked. The detailed process of hybrid MTDC grid startup schemes are presented in Fig. 5.1 and Fig. 5.2.

The first scheme with only two network zones inter-connected is shown in Fig. 5.1. This DC voltage is increased to 90% of its rated value as shown in Fig. 5.1 (a). To allow the DC power flow the AC voltages are provided to LCC's and MMC's ac sides of the converters, at time, $t = 0.2$ sec as shown in Fig. 5.1 (b). When MMC F1 (offshore rectifier) is unblocked at time, $t = 0.6$ sec the remaining DC voltage is ramped up to 100% of its rated as seen in Fig. 5.1 (c) and (a) respectively. Finally when the MMC E1 (offshore inverter connected to remote area load) is unblocked at 0.86 sec, the grid is now energized to supply power to all inverter sides' ac sources. All AC voltages and all DC currents starts building up as presented in Fig. 5.1 (b) and (c), the effects of integrating this converter can be seen in Fig. 5.1 (a) at 0.86 sec. Meanwhile the reactive powers calculated response at all these converters are shown in Fig. 5.1 (d), at 0.2 sec LCC's injecting reactive powers become stable.

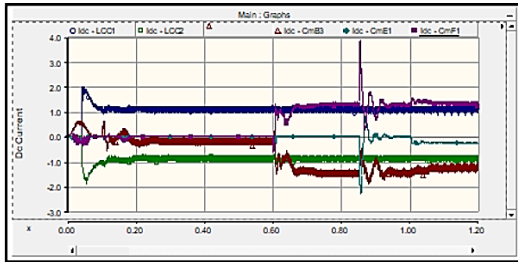
A second scheme is shown in Fig. 5.2 where all three network zones are integrated using DC-DC converters. Network zone 3 is used as an integration of DC sources into the system. Due to the initial inertia provided by the DC sources the DC current starts flowing earlier and DC voltage is ramped up to its 100% rated value at time, $t = 0.2$ sec as shown in Fig. 5.2 (c) and Fig. 5.2 (a). This allows the grid to energize beforehand and is able to continue the supply of DC Power to the required areas. In comparison with the previous scheme Fig. 5.2 (d) shows that the response of reactive powers of LCCs to converter changes is also stable than in Fig. 5.1 (d)



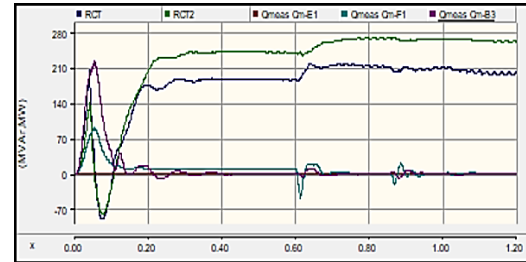
(a)



(b)

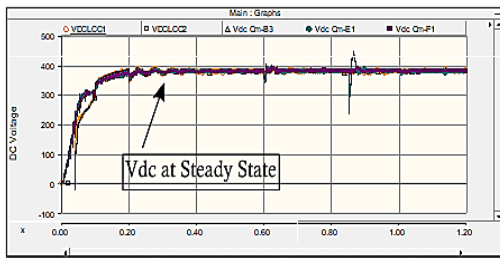


(c)

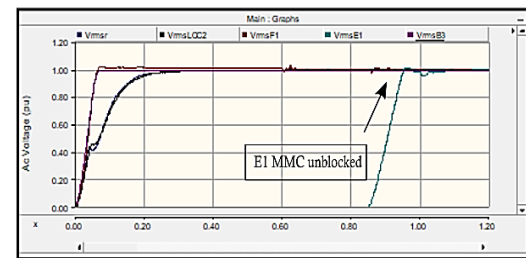


(d)

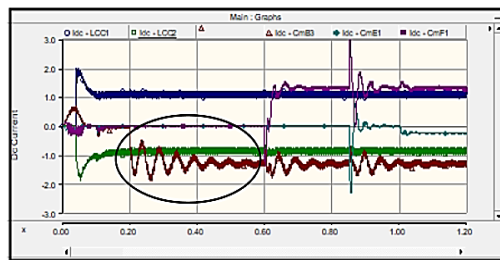
Figure 5.1: System response during start-up under normal conditions: (a) DC voltages (b) AC voltages (c) DC currents (d) reactive powers



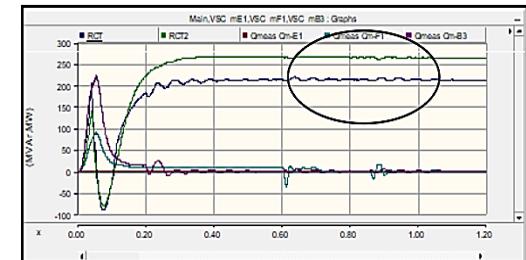
(a)



(b)



(c)



(d)

Figure 5.2: System response during start-up with DC source integration (a) DC voltages (b) AC voltages (c) DC currents

5.2 AC voltage Sags

There are basically three different types of AC faults introduced at different locations in the network zone 1 and 2. Their analysis is based on the response of the DC voltage, DC currents, active and reactive powers of the whole Hybrid grid. These faults create AC voltage sags at the converter sides. Firstly they are produced at the AC side of MMC F1 rectifier at time, $t = 1.2s$ for a time period of 200ms. These faults are of different nature and have slightly different impacts on the converters and the control strategies. An unbalance two phase to ground fault (70% AC voltage sags) creates an unbalance disturbance in the the DC voltages and currents of the DC grid which is much harder to resolve. Furthermore a balance three phase to ground fault (100% AC voltage sags) is also tested and the response of the system is compared using different topological schemes as discussed in the above section. The system have to be designed such that it is able to control and stabilize the grid under both types of these AC voltage sags. The performance of HMTDC grid voltages, currents and powers under the influence of these sags at MMC F1 are illustrated and discussed in Fig. 5.3, Fig. 5.4 and Fig. 5.5. Fig. 5.3 and 5.4 are used to compare the performance using scheme 1 and Fig. 5.3 and 5.5 are used to compare the performance using scheme 2.

During an unbalanced AC voltage sag shown in Fig. 5.3 (b) the AC voltage is fallen by 70% of the rated value that is from 1 per unit to 0.3 per unit for a time period of 200ms. The DC current feeded to the MMC B1 and MMC E1 inverters becomes almost null. Due to the isolation created in between the network zone by the DC-DC converters the DC currents of LLC rectifiers and inverters are unaffected by this fault which can be seen in Fig. 5.3 (c). In Fig. 5.3 (a) the DC voltage of the grid is affected by a peak 15.78% disturbance loss due to the distort nature of the fault. The quality of the DC voltage is also affected during the fault which is very dangerous for the electronic components of hybrid DC grid. When the converter is resumed after the fault at time = 1.4s, there are huge surges in reactive powers up to 550 Mvar which is there to lower the high currents of, up to 300% rated values, the converters as shown in Fig. 5.3 (d) and Fig. 5.3 (c). After time = 1.5s the hybrid grid becomes stable and power starts flowing.

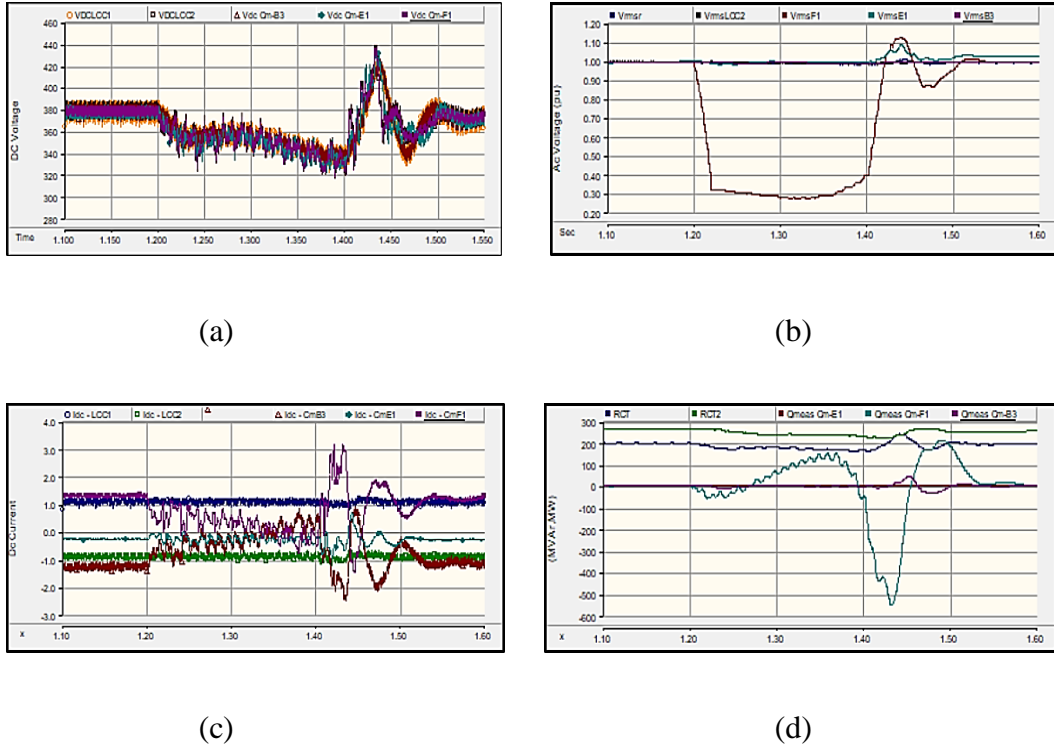


Figure 5.3: System response during unbalanced AC voltage Sags without DC source Integration: (a) DC voltages (b) AC voltages (c) DC currents (d) reactive powers.

A 100% voltage sag is created using a balanced three phase to ground AC fault as displayed in Fig. 5.4 (b). The fault is produced at time $t = 1.24s$ for a time span of 200ms and is cleared after time, $t = 1.44s$. IGBT's are used to block the high DC currents during the fault period of 100ms after that the AC voltage of the converters starts to ramp up again and reaches its rated value in 100ms. The DC currents and reactive powers during the sags in both the schemes are analyzed and compared as shown in Fig. 5.3 (c and d) and Fig. 5.4 (c and d). The surges in DC currents and reactive power requirements after the post fault at 1.44s are less in the second scheme. That is because the AC voltage ramps up to its rated value rapidly and reaches stability. Fig. 5.4 (a) also predicts that there is low distortion in the DC voltage and therefore voltage quality is maintained during and after the fault. Moreover the details of the effects of three types AC voltage sags at four converters applied at both the network zones are specified below in the Table 5.

Table. 4: Max change in DC voltage and Peak increase in AC current at 4 converters.

AC Sag Applied At Converter	Type of Disturbance	Max % Change in DC voltage during fault	Peak Increase in AC current
LCC Rectifier	30 % AC voltage Sag	±7.31%	6pu
	70 % AC voltage Sag	±6.17%	8pu
	100 % AC voltage Sag	±7.31%	12.5pu
MMC Inverter B3	30 % AC voltage Sag	±9.52%	6pu
	70 % AC voltage Sag	±26.34%	10pu
	100 % AC voltage Sag	±21.05%	9pu
MMC Inverter E1	30 % AC voltage Sag	±28.91%	8pu
	70 % AC voltage Sag	±31.64%	10pu
	100 % AC voltage Sag	±26.32%	7.5pu
MMC Rectifier F1	30 % AC voltage Sag	±7.89%	15pu
	70 % AC voltage Sag	±15.78%	17pu
	100 % AC voltage Sag	±15.78%	17pu

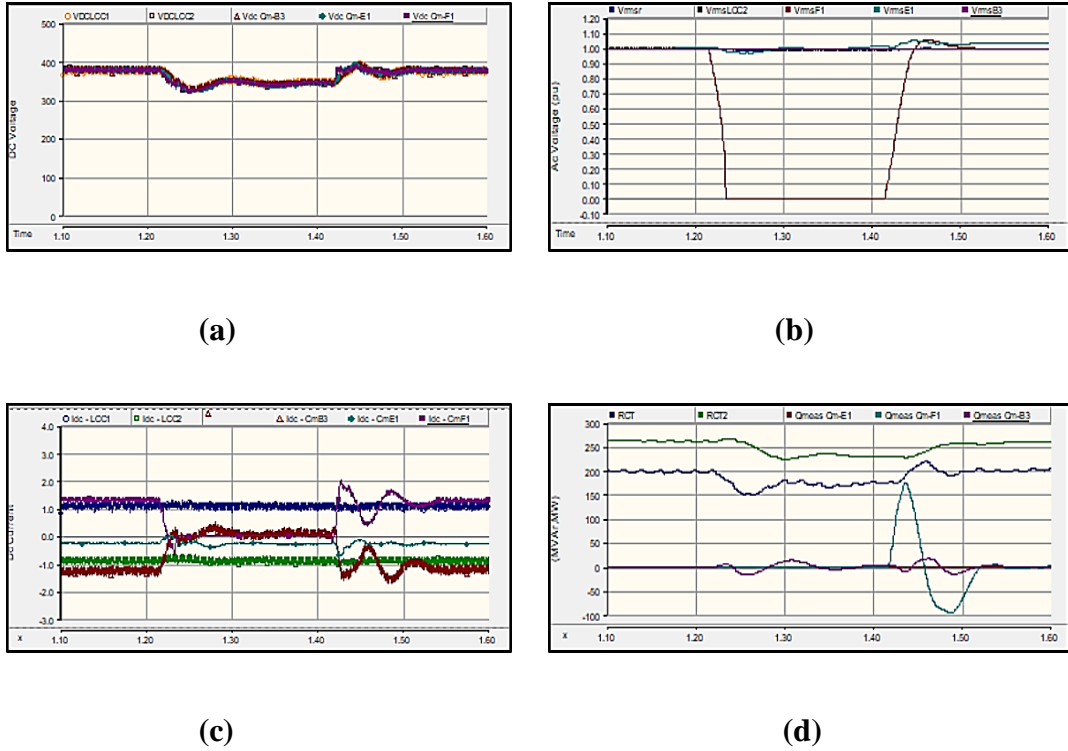


Figure 5.4: System response during balanced AC voltage Sags without DC source Integration: (a) DC voltages (b) AC voltages (c) DC currents (d) reactive powers.

The scheme two is used to represent the performance of hybrid MTDC grid as shown in Fig. 5.5 under unbalanced voltage sag conditions and compared with scheme one as shown in Fig. 5.3. The impacts of integrating a DC source using DC-DC converters can be seen from Fig. 5.5 (a) and Fig. 5.5 (c). A two phase to ground unbalanced AC voltage sag is introduced at time, $t = 1.2$ s and is cleared after 100ms. The DC voltage of the grid is slightly affected during this fault due to the inertia provided by the DC sources to MMC B3 inverter. This is required as the MMC F1 is blocked under faulty state. This puts less stresses on all the other converters and shields the internal components from overheating and will burden less on the controllers. The DC voltage presented in Fig. 5.5 (a) is nearly stable during the fault as compared to the DC voltage presented in Fig. 5.3 (a). The peak reactive power used up by the converter is also abridged by 58%. The Peak reactive power in Fig. 5.5 (d) is curtailed to 230Mvar. This shows that due to the stable DC voltages, the faults are impervious to propagation in network zone 1.

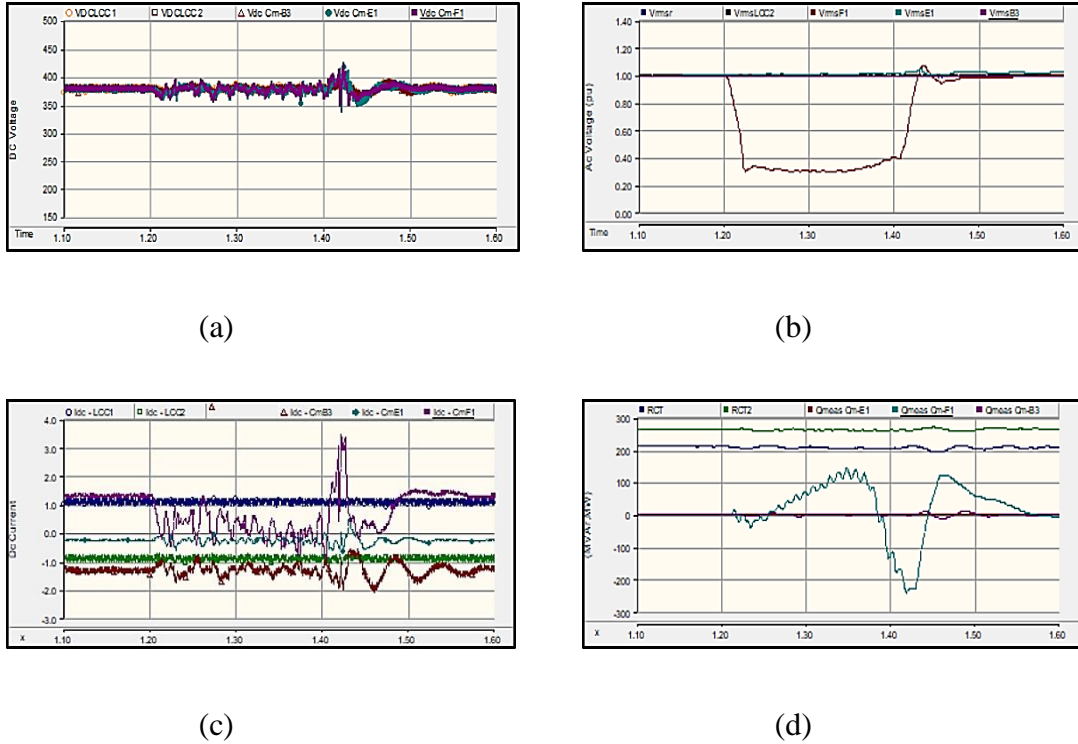


Figure 5.5: System response during start-up unbalanced AC voltage Sags with DC source Integration: (a) DC voltages (b) AC voltages (c) DC currents (d) reactive powers.

5.3 DC voltage Sags

Single line to line DC fault is used to produce a pole to pole DC voltage sag created at time, $t = 1.2s$ and is removed after 100ms. This sag is produced at DC lines near onshore MMC B3 inverter and offshore MMC F1 rectifier. The effects of this type of sags at multiple locations are being explored for the development of operational characteristics of hybrid MTDC grid. Some limitations regarding these sags include system recovery process, integration topologies for hybrid inter-connections and high currents and reactive power requirements. These limitations are discussed and explored further.

Fig. 5.6 and Fig. 5.7 displays the performance of the hybrid MTDC grid system during DC voltage sags at the inverter MMC B3 and the rectifier MMC F1 respectively in zone 2. At time, $t = 1.2s$ a DC voltage sag for 100ms is produced firstly near inverter MMC B3. This results in a 100% drop of DC voltage as displayed in Fig. 5.6 (a). In Fig. 5.6 (b) The AC voltage of remote area load inverter MMC E1 (V_{rmsE1}) is set to

zero till the fault is gone. This gradually increases for time $t = 0.2s$ to protect the system.

The DC current due to this DC voltage sag rises sharply to treacherous values which are highly troublesome for the converter equipment consequently all MMCs are blocked as shown in Fig. 5.7(c) and (d). The DC voltages and AC voltage shown in Fig. 5.6 (a) and Fig. 5.6 (b) regain its steady state in time, $t = 0.3s$ after the fault is removed, whereas the DC voltages and AC Voltages in case two takes time, $t = 0.5s$ to reach its rated value as shown in Fig. 5.7 (a) and Fig. 5.7 (b). This happens because of the distance of sag applied is different in both the cases.

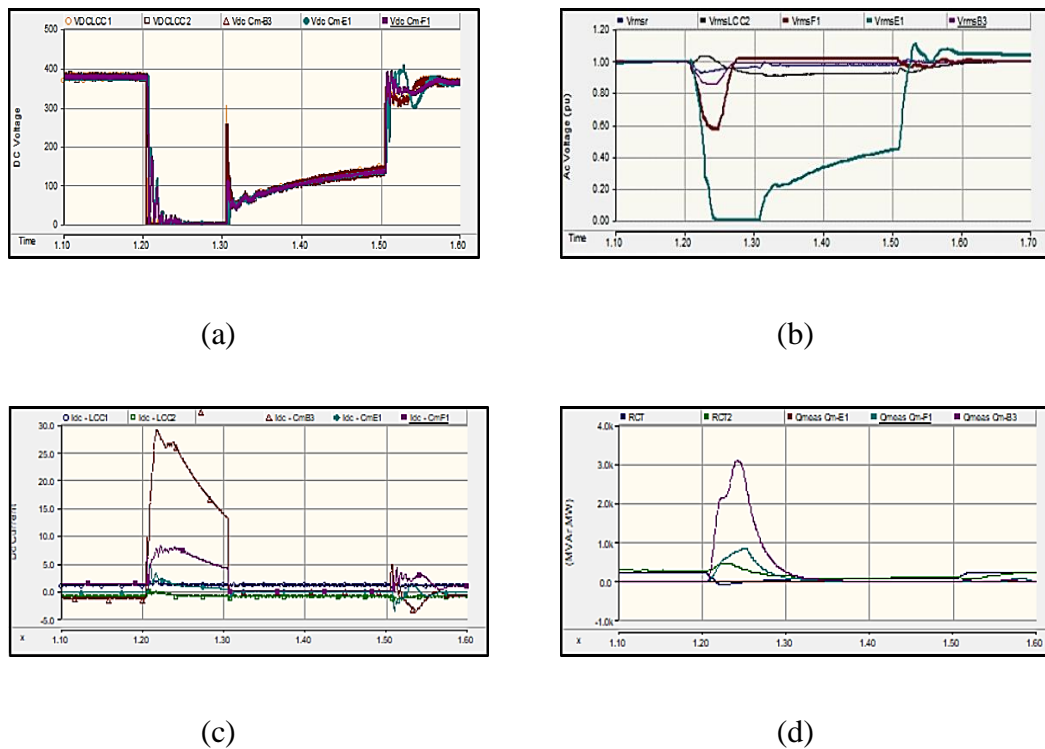
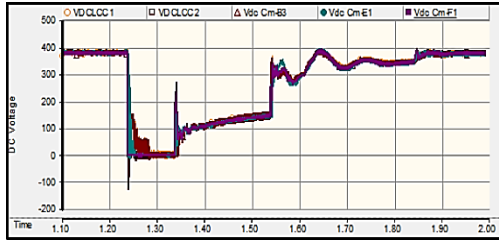
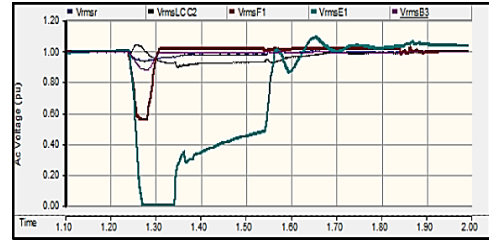


Figure 5.6: System response during DC voltage Sags at B3 (a) DC voltages (b) AC voltages (c) DC currents (d) reactive powers



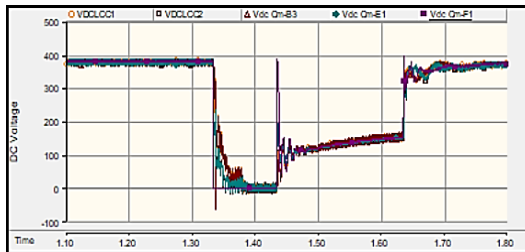
(a)



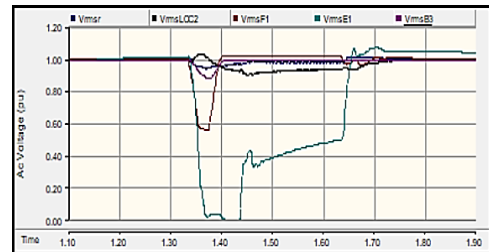
(b)

Figure 5.7: System response during DC voltage Sags at F1: (a) DC voltages (b) AC voltages

Fig. 5.8 presents the results of DC voltage sag produced at rectifier MMC F1 where hybrid inter-connection is made via dc line near MMC E1 (remote area load converter) to investigate the impacts of DC voltage sags using multiple topologies on operational characteristics of hybrid MTDC grid system. The DC voltage recovery time improved by time, $t = 0.2s$ as shown in Fig. 5.8 (a) and (b) in comparison with Fig. 5.7 (a) and (b).



(a)



(b)

Figure 5.8: System response during DC voltage Sags at F1 (Connection Topology)
(a) DC voltages (b) AC voltages.

Chapter 6: Conclusion

A Hybrid MTDC system provides numerous applications and advantages for the interconnection of different types of AC and DC grids, with diversity in integrating multiple resources and loads with higher controllability, stability, reliability and economy. This system is best suited for interconnecting clean energy from the sea to the load requirements of the land and vice versa. Most of the HMTDC systems are under exploration phase and still requires satisfactory research analysis for different case studies. This research work had the objectives of analyzing multiple approaches to improve the overall stability of the grid voltages and currents by understanding the behavior of the complete system under different abnormal conditions, which included single phase to ground faults, double phase to ground faults, triple phase to ground faults at the ac sides of the HVDC converters and pole to pole dc faults on dc sides of the HVDC converters. Further analysis had the objective of investigation on the topology of hybrid grid. Last but not the least goal of this thesis was to investigate and compare the overall performance of the proposed system under the use of DC-DC converters and DC sources with the above mentioned objectives. The system performance during startup, and under all above mentioned abnormal circumstances during steady state grid conditions shows better results while comparison with and without the integration of dc sources in the system. The hybrid was likely capable of handling most of these faults and the topological analysis clearly showed the disadvantage of interconnecting LCC converter with MMC's load area side converter, reducing the overall efficiency of the grid by impacting the fault handling capabilities.